

# Improved Correlations for Threshold Flooding and Entrainment in Sieve Trays in Distillation/Absorption Columns

Aline R. C. Souza, Miguel J. Bagajewicz, and André L. H. Costa\*



Cite This: *Ind. Eng. Chem. Res.* 2025, 64, 2256–2273



Read Online

ACCESS |



Metrics & More

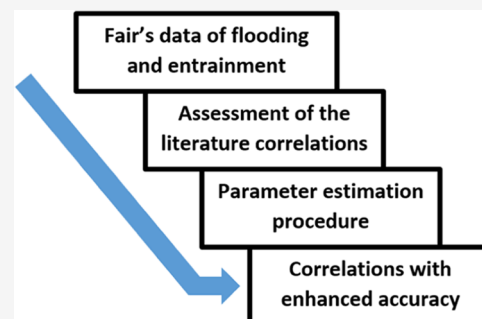


Article Recommendations



Supporting Information

**ABSTRACT:** The design of tray distillation/absorption columns involves the utilization of tray evaluation procedures. These procedures are based on flooding and entrainment data originally available in graphs (Souders–Brown flooding constant,  $C_{sb}$ , and fractional entrainment,  $\psi$ ). Aiming at using these data for computational applications, several algebraic correlations were proposed in the literature. However, a comparison of the predictions of these correlations and the original data reported by Fair (1961) indicates considerable deviations, which can compromise the accuracy of computational tools that use these expressions. In this article, a new set of parameters is determined for these correlations through reestimation of the correlation parameters using modern optimization techniques and the splitting of the correlation domain in multiple regions. The new set of parameters provides a significant reduction in the prediction errors. To demonstrate the importance of the utilization of the revised set of parameters, a comparison is made of column design results using the original and new parameters. The comparison indicates that the use of low-accuracy options affects the design, which can yield infeasible solutions. The evidence of design problems associated with the correlations is available in the literature, emphasizing the importance of the new set of parameters presented here.



## 1. INTRODUCTION

The design of sieve trays in distillation/absorption columns is usually performed by checking proposed geometries for their performance using several hydraulic extremes, namely, flooding, entrainment, weeping, downcomer choking, and residence time.<sup>1–3</sup> Some of these tests are based on data that were originally presented in the form of graphs. In this article, we are concerned with two issues: flooding and entrainment.

The use of computers for process equipment design demanded the adoption of equations to represent the data employed in tray design instead of manual data extraction from graphs. Thus, several correlations attempting to fit the data from these graphs into different expressions as a function of the independent variables were developed.

Correlations for the flooding graphical information presented by Fair<sup>4</sup> (also reproduced in Fair,<sup>5</sup> Coulson et al.,<sup>6</sup> and Kister et al.<sup>7</sup>) were proposed by Economopoulos,<sup>8</sup> Lygeros and Magoulas,<sup>9</sup> Kessler and Wankat,<sup>10</sup> and Ogboja and Kuye.<sup>11</sup> In turn, correlations for entrainment were proposed by Economopoulos,<sup>8</sup> Lygeros and Magoulas,<sup>9</sup> and Ogboja and Kuye.<sup>11</sup> Later, these correlations were employed by many authors involving different separation systems and problems.

The correlations proposed by Economopoulos<sup>8</sup> were employed for the hydraulic design of CO<sub>2</sub> and H<sub>2</sub>S absorbers.<sup>12</sup> The correlations proposed by Lygeros and Magoulas<sup>9</sup> were employed in investigations of the interactions between optimal design and control, involving double-effect distillation,<sup>13</sup> reactive distillation,<sup>14,15</sup> and multicomponent distillation.<sup>16</sup>

These correlations were also used for the analysis of other separation systems, such as supercritical fluid extraction,<sup>17</sup> high-pressure separation of carbon dioxide and methane,<sup>18</sup> dehydration of natural gas using triethylene glycol,<sup>19</sup> and azeotropic separation processes with ionic liquids.<sup>20</sup> The correlation of Kessler and Wankat<sup>10</sup> for flooding was used for modeling an ammonia absorber of an ammonia–water refrigeration cycle.<sup>21</sup> The liquid entrainment correlation of Ogboja and Kuye<sup>11</sup> was employed for the nonequilibrium modeling of multicomponent separation processes.<sup>22</sup> More recently, the correlations of Ogboja and Kuye<sup>11</sup> were employed in the optimal design of sieve plates using mixed-integer nonlinear programming.<sup>23</sup>

The accuracy of the results from the papers mentioned above depends on the accuracy of the employed correlations. Therefore, it is important to evaluate how close the correlation predictions are to the original Fair's data and try to reduce the corresponding errors. The availability of more accurate predictions is important for future works on the analysis and

**Received:** August 19, 2024

**Revised:** December 16, 2024

**Accepted:** December 18, 2024

**Published:** January 15, 2025



**Table 1. Parameters of the Correlations of Economopoulos,<sup>8</sup> Lygeros and Magoulas,<sup>9</sup> and Ogboja and Kuye<sup>11</sup>**

Correlation	$\theta_{C_{sb}1}$	$\theta_{C_{sb}2}$	$\theta_{C_{sb}3}$	$\theta_{C_{sb}4}$	$\theta_{C_{sb}5}$	$\theta_{C_{sb}6}$
Economopoulos <sup>8</sup>	0.118	0.0479	0.425	0.0479	0.1092	−0.058
Lygeros and Magoulas <sup>9</sup>	0.0105	0.1496	0.755	1.463	0.842	
Ogboja and Kuye <sup>11</sup>	0.0129	0.1674	0.0063	−0.2686	−0.008	0.1448

optimization of distillation and absorption columns using computational tools.

According to these needs, we compare in this article the correlation predictions with Fair's data set, identifying the errors associated with each alternative and providing more accurate options based on the same correlations. The reduction of the errors associated with these correlations was attained by a re-evaluation of the correlation parameters through the solution of parameter estimation problems using modern optimization algorithms. The split of the correlation domain and the estimation of the parameters for each resultant region were also employed to provide more accurate results. It is important to observe that the original correlations were published from 1978 until 1990, i.e., the original parameters were determined using older optimization tools, which can explain the accuracy problems shown in this paper (according to our knowledge, there are no newer alternatives of correlations available in the literature).

The current article is organized as follows. Section 2 presents the published correlations of flooding and entrainment associated with an analysis of the corresponding errors in the context of the original data from Fair.<sup>4</sup> Section 3 presents the objective function for the estimation of the parameters. Section 4 presents the results of the parameter estimation of the correlations applied in this paper. Section 5 illustrates the application of the correlations to the original and new parameters for the design of distillation columns. The conclusions are finally presented in Section 6.

## 2. ACCURACY OF THE CORRELATIONS AVAILABLE IN THE LITERATURE

To determine the accuracy of the models found in the literature, we obtained numerical values of Fair's curves using the Engauge

**Table 2. Parameters of the Correlation of Kessler and Wankat,<sup>10</sup> Quadratic Expression**

Tray spacing (in)	$\theta_{C_{sb}1}$	$\theta_{C_{sb}2}$	$\theta_{C_{sb}3}$
6	1.1977	0.53143	0.18760
9	1.1622	0.56014	0.18168
12	1.1175	0.61567	0.19510
18	1.0262	0.63513	0.20097
24	0.94506	0.70234	0.22618
36	0.85984	0.73980	0.23735

Digitizer software version 4.1<sup>24</sup> and calculated the errors of the correlations proposed to fit the original curves. The data collection corresponds to 328 points about flooding and 379 points about entrainment, individually reported in the Supporting Information (Section S1).

**2.1. Flooding Correlations.** A flooding correlation usually determines the limiting velocity of the vapor (uflood) in the active zone. In tray rating/design, the following constraint is used:<sup>3</sup>

$$un \leq 0.85uflood \quad (1)$$

**Table 3. Parameters of the Correlation of Kessler and Wankat,<sup>10</sup> Cubic Expression**

Tray spacing (in)	Flv	$\theta_{C_{sb}1}$	$\theta_{C_{sb}2}$	$\theta_{C_{sb}3}$	$\theta_{C_{sb}4}$
6	≤0.1	0.858	0.0398	0.148	0.112
9		0.744	0.0598	0.100	0.0891
12		0.646	0.00908	0.00179	0.0509
18		0.538	0.0281	0.0319	0.0681
24		0.420	0.0294	0.0636	0.0918
36		0.301	0.0340	0.0389	0.0751
6	>0.1	0.862	0.0808	0.189	0.0515
9		0.793	0.127	0.167	0.0605
12		0.708	0.165	0.155	0.0729
18		0.602	0.169	0.172	0.0673
24		0.478	0.178	0.212	0.0623
36		0.371	0.181	0.186	0.0985

**Table 4. Errors of the Flooding Correlation by Economopoulos<sup>8</sup>**

Tray spacing (in)	Average error (%)	Maximum error (%)
6	9.09	21.98
9	5.44	15.76
12	4.32	18.48
18	5.56	37.99
24	8.38	53.82
36	52.33	85.06

**Table 5. Errors of the Flooding Correlation by Lygeros and Magoulas<sup>9</sup>**

Tray spacing (m)	Average error (%)	Maximum error (%)
0.1524	5.02	15.90
0.2286	5.05	21.52
0.3048	4.24	13.26
0.4572	4.56	15.09
0.6096	3.12	6.67
0.9144	2.51	4.57

**Table 6. Errors of the Flooding Correlation by Ogboja and Kuye<sup>11</sup>**

Tray spacing (m)	Average error (%)	Maximum error (%)
0.1524	12.78	15.17
0.2286	10.76	208.61
0.3048	11.48	290.24
0.4572	16.39	433.40
0.6096	17.40	504.05
0.9144	14.97	20.71

This correlation states that the velocity (un) of the vapor in the active zone must be below 85% of the flooding velocity (uflood). In turn, the flooding velocity is given by:

$$uflood = KC_{sb} \sqrt{\frac{\rho l - \rho v}{\rho v}} \left( \frac{\sigma}{0.02} \right)^{0.2} \quad (2)$$

**Table 7. Errors of the Flooding Quadratic Correlation by Kessler and Wankat<sup>10</sup>**

Tray spacing (in)	Average error (%)	Maximum error (%)
6	4.47	7.81
9	5.10	9.79
12	7.43	25.59
18	5.06	15.27
24	5.16	10.55
36	6.67	15.63

**Table 8. Errors of the Cubic Flooding Correlation by Kessler and Wankat<sup>10</sup>**

Tray spacing (in)	Average error (%)	Maximum error (%)
6	1.24	7.47
9	1.70	14.81
12	2.99	11.96
18	2.42	11.82
24	2.60	9.83
36	5.53	7.84

where  $\rho l$  and  $\rho v$  are the liquid and vapor densities, respectively,  $\sigma$  is the surface tension,  $K$  is a constant depending exclusively on the tray geometry, and  $C_{sb}$  is the Souders–Brown constant. The Souders–Brown constant depends on the tray spacing ( $lt$ ) and the liquid–vapor flow factor ( $Flv$ ):

$$Flv = \frac{L}{V} \sqrt{\frac{\rho v}{\rho l}} \quad (3)$$

where  $L$  and  $V$  are the liquid and vapor flow rates, respectively.

Fair<sup>4</sup> presented graphs from which one is supposed to extract the value of  $C_{sb}$ . Several correlations were proposed to obtain  $C_{sb}$  algebraically, where the parameter values were obtained by undisclosed methods (maybe nonlinear fitting): Economopoulos,<sup>8</sup> Lygeros and Magoulas,<sup>9</sup> Ogboja and Kuye,<sup>11</sup> and Kessler and Wankat.<sup>10</sup> These correlations are shown next according to the original units of  $lt$  and  $C_{sb}$  presented in the respective papers:

Economopoulos:<sup>8</sup>

$$C_{sb} \text{ (ft/s)} = \min[\theta_{C_{sb,1}} \exp(\theta_{C_{sb,2}} lt(\text{in})), \theta_{C_{sb,3}} \exp(\theta_{C_{sb,4}} lt(\text{in}))(\theta_{C_{sb,5}} + \theta_{C_{sb,6}} \ln Flv)] \quad (4)$$

Lygeros and Magoulas:<sup>9</sup>

$$C_{sb} \text{ (m/s)} = \theta_{C_{sb,1}} + \theta_{C_{sb,2}} [lt(\text{m})]^{\theta_{C_{sb,3}}} \exp(-\theta_{C_{sb,4}} Flv^{\theta_{C_{sb,5}}}) \quad (5)$$

Ogboja and Kuye:<sup>11</sup>

$$C_{sb} \left( \frac{\text{m}}{\text{s}} \right) = \theta_{C_{sb,1}} + \theta_{C_{sb,2}} lt(\text{m}) + \theta_{C_{sb,3}} Flv + \theta_{C_{sb,4}} lt(\text{m}) Flv + \theta_{C_{sb,5}} Flv^2 + \theta_{C_{sb,6}} lt(\text{m}) Flv^2 \quad (6)$$

Kessler and Wankat,<sup>10</sup> quadratic expressions:

$$\log_{10} C_{sb} \text{ (ft/s)} = -\theta_{C_{sb,1}} - \theta_{C_{sb,2}} \log_{10} Flv - \theta_{C_{sb,3}} (\log_{10} Flv)^2 \quad (7)$$

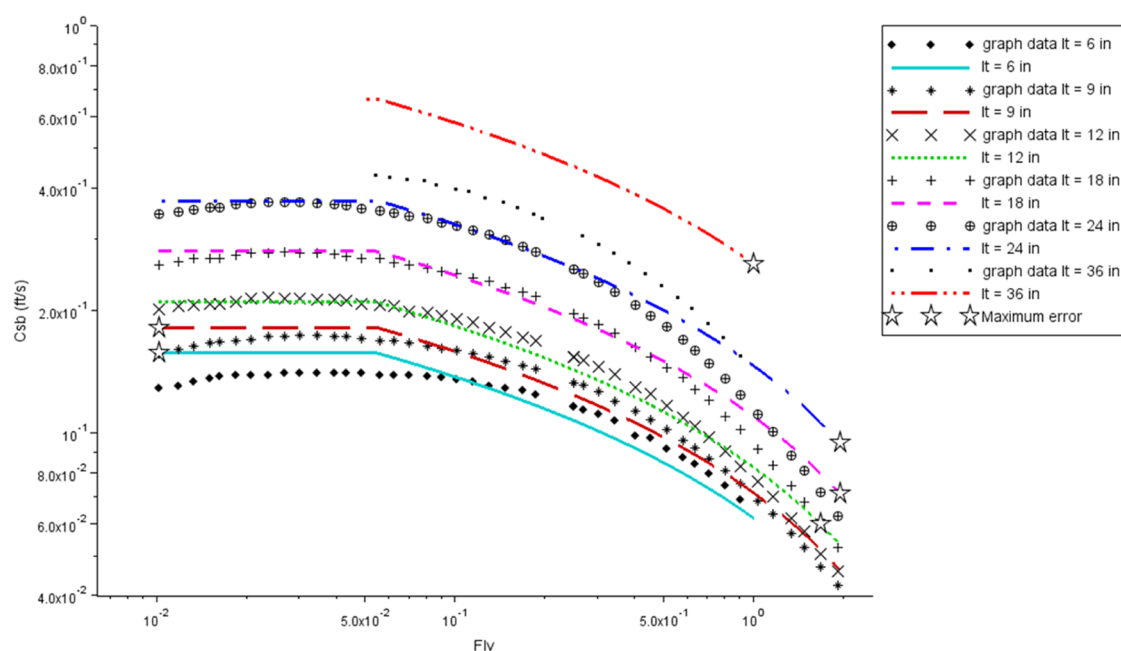
Kessler and Wankat,<sup>10</sup> cubic spline expressions:

For  $Flv \leq 0.1$ :

$$\log_{10} C_{sb} \text{ (ft/s)} = -\theta_{C_{sb,1}} - \theta_{C_{sb,2}} (\log_{10} Flv + 2) + \theta_{C_{sb,3}} (\log_{10} Flv + 2)^2 - \theta_{C_{sb,4}} (\log_{10} Flv + 2)^3 \quad (8)$$

For  $Flv > 0.1$ :

$$\log_{10} C_{sb} \text{ (ft/s)} = -\theta_{C_{sb,1}} - \theta_{C_{sb,2}} (\log_{10} Flv + 1) + \theta_{C_{sb,3}} (\log_{10} Flv + 1)^2 - \theta_{C_{sb,4}} (\log_{10} Flv + 1)^3 \quad (9)$$

**Figure 1.** Comparison of the original data of the Souders–Brown constant with the correlation proposed by Economopoulos.<sup>8</sup>

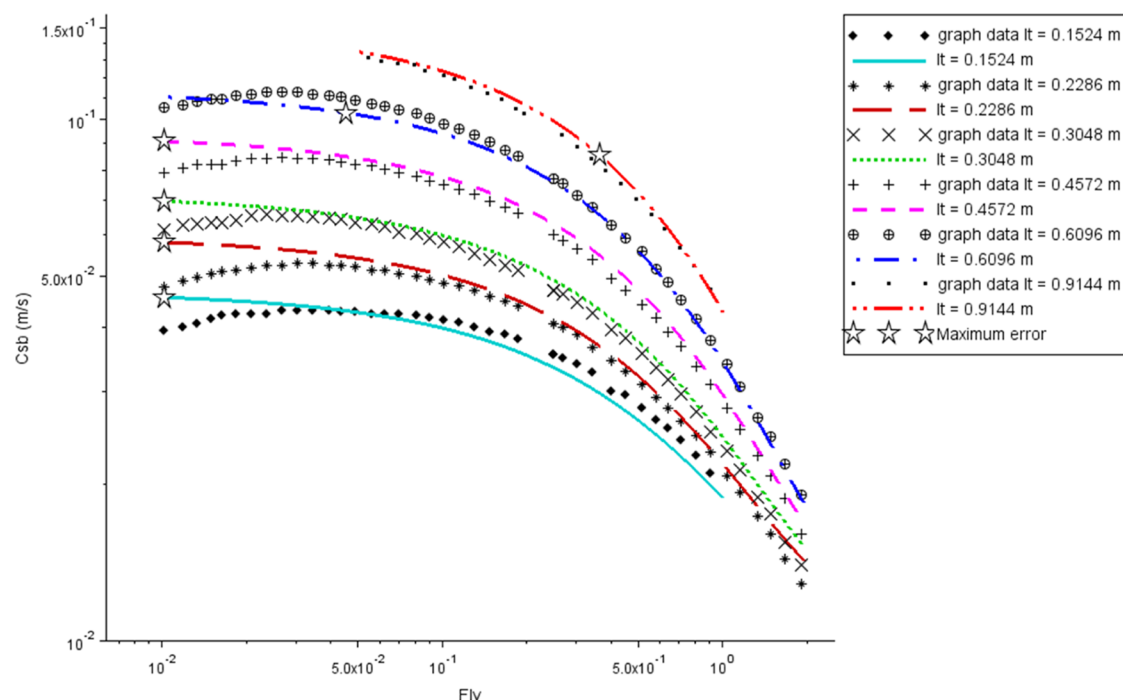


**Figure 2.** Comparison of the original data of the Souders–Brown constant with the correlation proposed by Lygeros and Magoulas.<sup>9</sup>

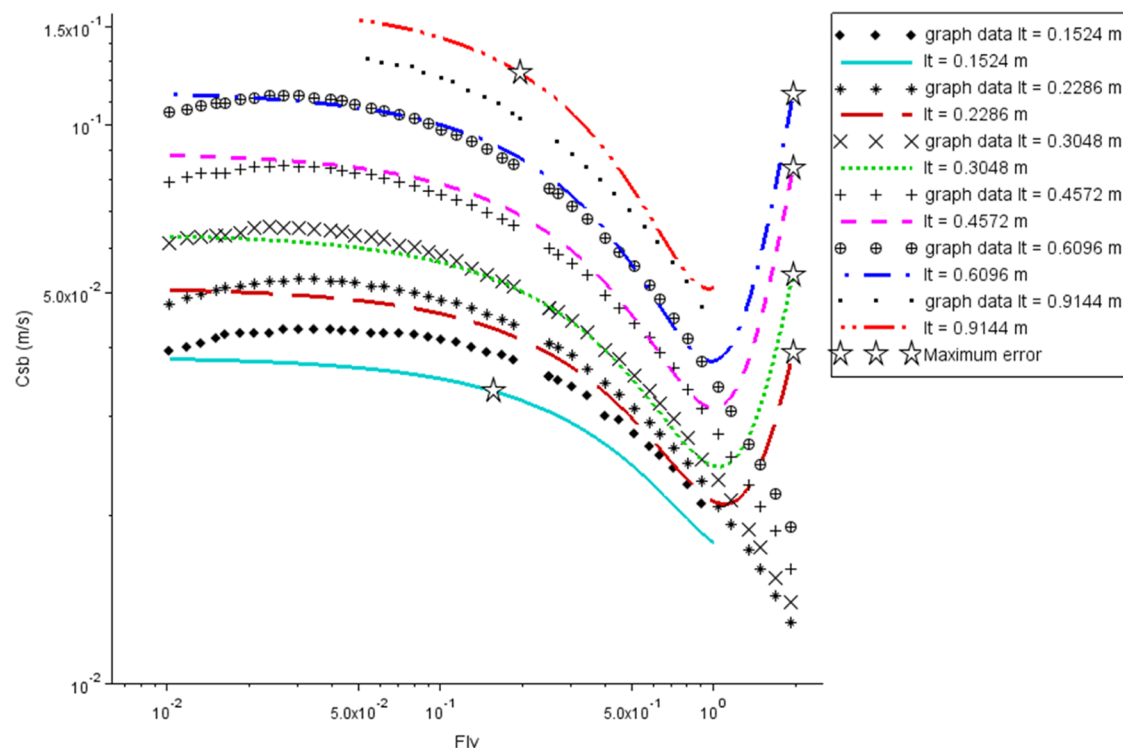


**Figure 3.** Comparison of the original data of the Souders–Brown constant with the correlation proposed by Ogboja and Kuye.<sup>11</sup>

where  $\theta_{C_{sb},k}$  for  $k = 1, \dots, 6$ , are correlation parameters, displayed in Tables 1–3 (the parameters of the quadratic and cubic correlations of Kessler and Wankat<sup>10</sup> depend on the tray spacing and the parameters of the cubic correlation also depend on the  $Flv$  range).

Tables 4–8 present the errors of the correlations proposed by Economopoulos,<sup>8</sup> Lygeros and Magoulas,<sup>9</sup> Ogboja and Kuye,<sup>11</sup> and Kessler and Wankat,<sup>10</sup> respectively, as compared to the data

extracted from the original Fair's graph<sup>4</sup> (the values of tray spacing are depicted in these tables according to the original units of the correlation):

Figures 1–5 show the points of the data extracted from the original curve and the curves of the correlations of Economopoulos,<sup>8</sup> Lygeros and Magoulas,<sup>9</sup> Kessler and Wankat,<sup>10</sup> and Ogboja and Kuye.<sup>11</sup> The original set of points was reduced from 328 to 45 in these figures for better visualization. The points associated with the maximum errors



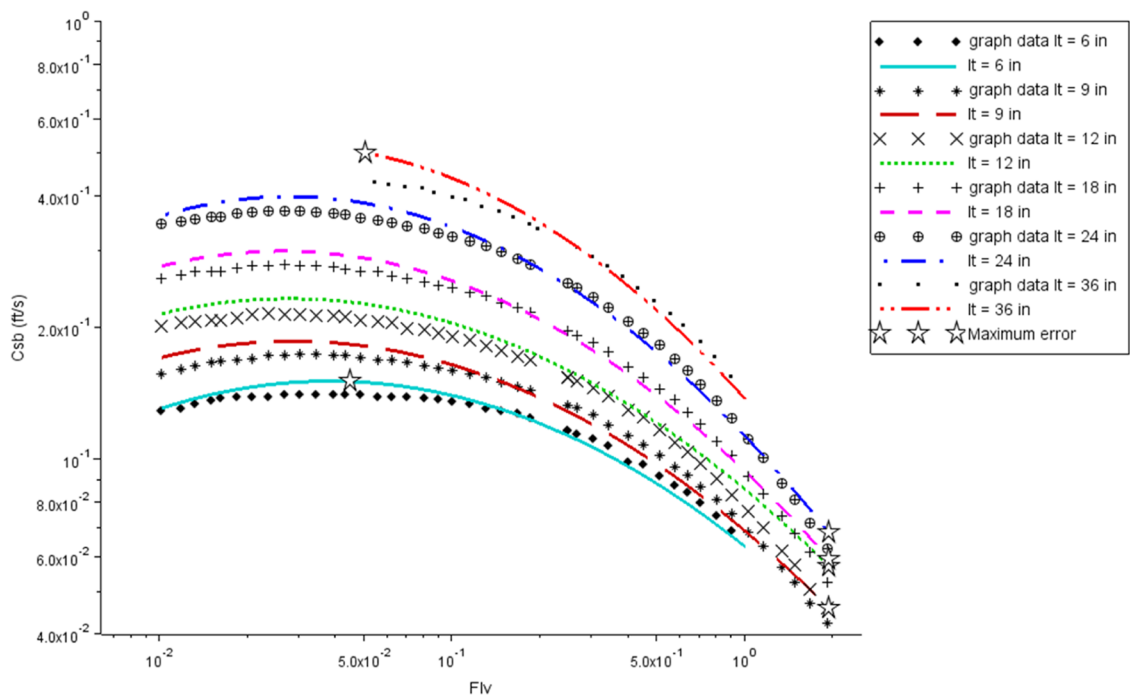


**Figure 4.** Comparison of the original data of the Souder–Brown constant with the quadratic correlation proposed by Kessler and Wankat.<sup>10</sup>

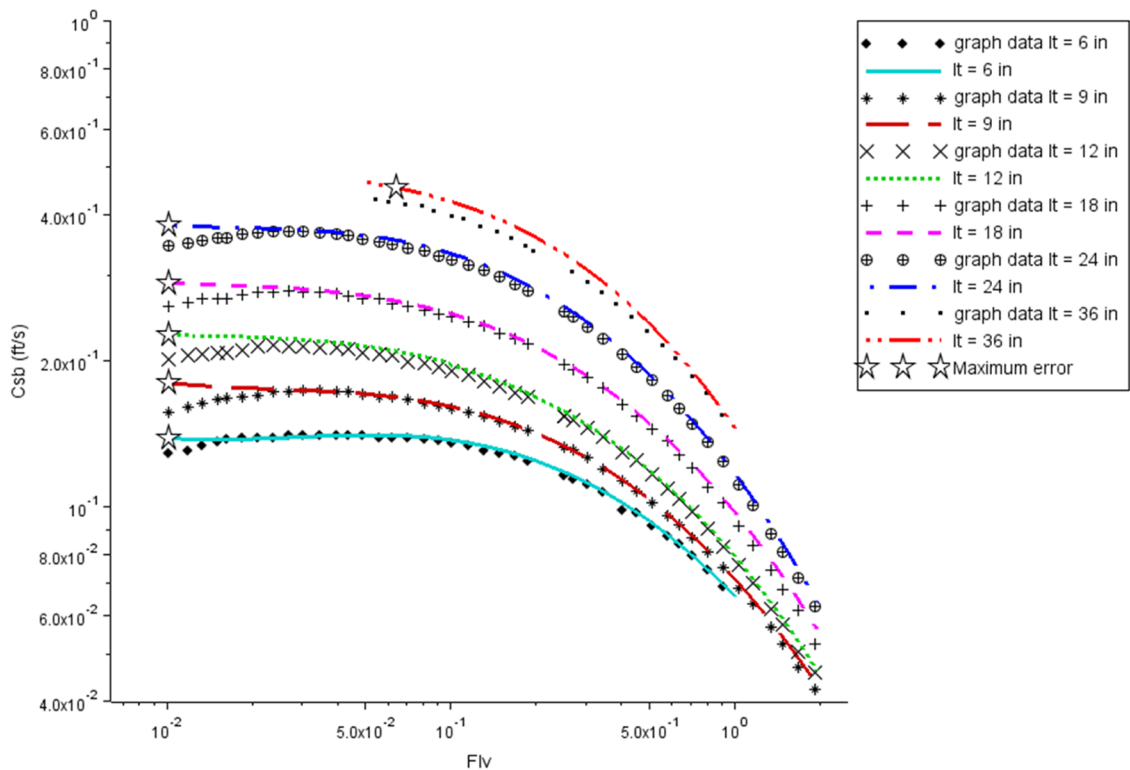


**Figure 5.** Comparison of the original data of the Souder–Brown constant with the cubic correlation proposed by Kessler and Wankat.<sup>10</sup>

**Table 9.** Parameters of the Correlations of Economopoulos<sup>8</sup> and Ogboja and Kuye<sup>11</sup> for Evaluation of the Fractional Entrainment

Correlation	$\theta_{\psi,1}$	$\theta_{\psi,2}$	$\theta_{\psi,3}$	$\theta_{\psi,4}$	$\theta_{\psi,5}$	$\theta_{\psi,6}$	$\theta_{\psi,7}$	$\theta_{\psi,8}$
Economopoulos <sup>8</sup>	6.692	1.956	−0.132	0.654				
Ogboja and Kuye <sup>11</sup>	−7.9196	1.0891	0.0705	2.1916	0.046	−0.605	1.2699	−0.9563

**Table 10. Parameters of the Correlation of Lygeros and Magoulas<sup>9</sup> for Evaluation of the Fractional Entrainment**

Fractional flooding (%)	$\theta_{\psi,1}$	$\theta_{\psi,2}$	$\theta_{\psi,3}$	$\theta_{\psi,4}$
90	$0.517 \times 10^{-2}$	1.050	−10.837	0.511
80	$0.224 \times 10^{-2}$	2.377	−9.394	0.314
70	$-0.509 \times 10^{-3}$	81.82	−11.389	0.1317
60	$-0.868 \times 10^{-3}$	1537.05	−14.205	0.0828

**Table 11. Errors of the Entrainment Correlations by Economopoulos<sup>8</sup>**

Fractional flooding (%)	Average error (%)	Maximum error (%)
90	20.73	42.68
80	26.99	48.38
70	28.94	50.60
60	22.88	32.24
50	6.23	13.61
45	5.48	8.34
40	2.95	5.79
35	3.87	15.35
30	9.49	31.56

**Table 12. Errors of the Entrainment Correlations by Lygeros and Magoulas<sup>9</sup>**

Fractional flooding (%)	Average error (%)	Maximum error (%)
90	15.26	42.88
80	14.61	37.60
70	14.54	44.68
60	12.88	27.52

**Table 13. Errors of the Entrainment Correlations by Ogboja and Kuye<sup>11</sup>**

Fractional flooding (%)	Average error (%)	Maximum error (%)
90	9.02	23.69
80	34.37	75.84
70	36.24	82.41
60	19.27	29.17
50	7.18	24.22
45	8.26	26.15
40	5.69	16.22
35	1.54	4.73
30	23.63	47.92

of each correlation are marked in the graph to provide an identification of the regions with higher deviations between the correlation and the original data.

The analysis of the accuracy of each correlation indicates the presence of large errors, which can compromise the results of computational applications that use these correlations.

The correlation of Economopoulos<sup>8</sup> presents lower accuracy for larger values of tray spacing. It is possible to observe in Figure 1 that the results of this correlation are far from the Fair's data along the entire data set of the 36 in tray spacing (the maximum error here is 85.06%).

The correlation of Lygeros and Magoulas<sup>9</sup> is more accurate, with a maximum error of 21.52% (but it is still considerably large). Figure 2 indicates that the higher deviations are concentrated in the data with smaller values of Flv.

The correlation of Ogboja and Kuye<sup>11</sup> presents average errors higher than the correlations of Economopoulos<sup>8</sup> and Lygeros and Magoulas.<sup>9</sup> The maximum errors are particularly high because the profile of the curves for large values of Flv is in an

opposite trend when compared with the Fair's data, as can be observed in Figure 3.

The correlation of Kessler and Wankat<sup>10</sup> based on a cubic expression presents a better performance than the quadratic expression. The average errors are the smallest ones compared with the other correlations, but there are errors up to 14.81%. The best performance of this correlation can be explained by the separation of the domain in different regions of tray spacing and Flv. Additionally, the Kessler and Wankat<sup>10</sup> correlation is only available for the discrete values of tray spacing reported in Fair<sup>4</sup> (the dependency with the tray spacing in the other correlations is explicitly included in the mathematical expression).

**2.2. Entrainment Correlations.** Entrainment in sieve trays is controlled by limiting the fractional entrainment ( $\psi$ ), which is defined as the fraction of liquid carried to the tray above by the vapor. Typically, this limit corresponds to the following constraint, employed in rating/design procedures:<sup>3</sup>

$$\psi(\text{Flood}) \leq 0.1 \quad (10)$$

where Fflood is the fractional flooding, in turn, defined by:

$$\text{Fflood} = \frac{u_n}{u_{\text{flood}}} \quad (11)$$

Economopoulos,<sup>8</sup> Lygeros and Magoulas,<sup>9</sup> and Ogboja and Kuye<sup>11</sup> proposed the following correlations:

$$\psi = \exp[-(\theta_{\psi,1} + \theta_{\psi,2}\text{Fflood})\text{Flv}^{(\theta_{\psi,3} + \theta_{\psi,4}\text{Fflood})}] \quad (12)$$

Lygeros and Magoulas:<sup>9</sup>

$$\psi = \theta_{\psi,1} + \theta_{\psi,2} \exp[\theta_{\psi,3}\text{Flv}^{(\theta_{\psi,4})}] \quad (13)$$

Ogboja and Kuye:<sup>11</sup>

$$\psi = \exp[\theta_{\psi,1} + \theta_{\psi,2}\text{Fflood} - (\theta_{\psi,3} + \theta_{\psi,4}\text{Fflood})\ln(\text{Flv}) + (\theta_{\psi,5} + \theta_{\psi,6}\text{Fflood} + \theta_{\psi,7}\text{Fflood}^2 + \theta_{\psi,8}\text{Fflood}^3)(\ln(\text{Flv}))^2] \quad (14)$$

where  $\theta_{\psi,k}$  for  $k = 1, \dots, 8$ , are correlation parameters (the parameters of the correlation of Lygeros and Magoulas<sup>9</sup> depend on discrete values of fractional flooding), as depicted in Tables 9 and 10.

Tables 11–13 present the errors of the models of Economopoulos,<sup>8</sup> Lygeros and Magoulas,<sup>9</sup> and Ogboja and Kuye<sup>11</sup> as compared to the data extracted from the original Fair's graph.

Figures 6–8 show the points of the data extracted from the original Fair's graph and the curves of the models of Economopoulos,<sup>8</sup> Lygeros and Magoulas,<sup>9</sup> and Ogboja and Kuye.<sup>11</sup> The original points in these figures were reduced from 380 to 50 points for better visualization. The points associated with the maximum errors of each correlation are marked in the graph to provide an identification of the regions with higher deviations between the correlations and the original data.

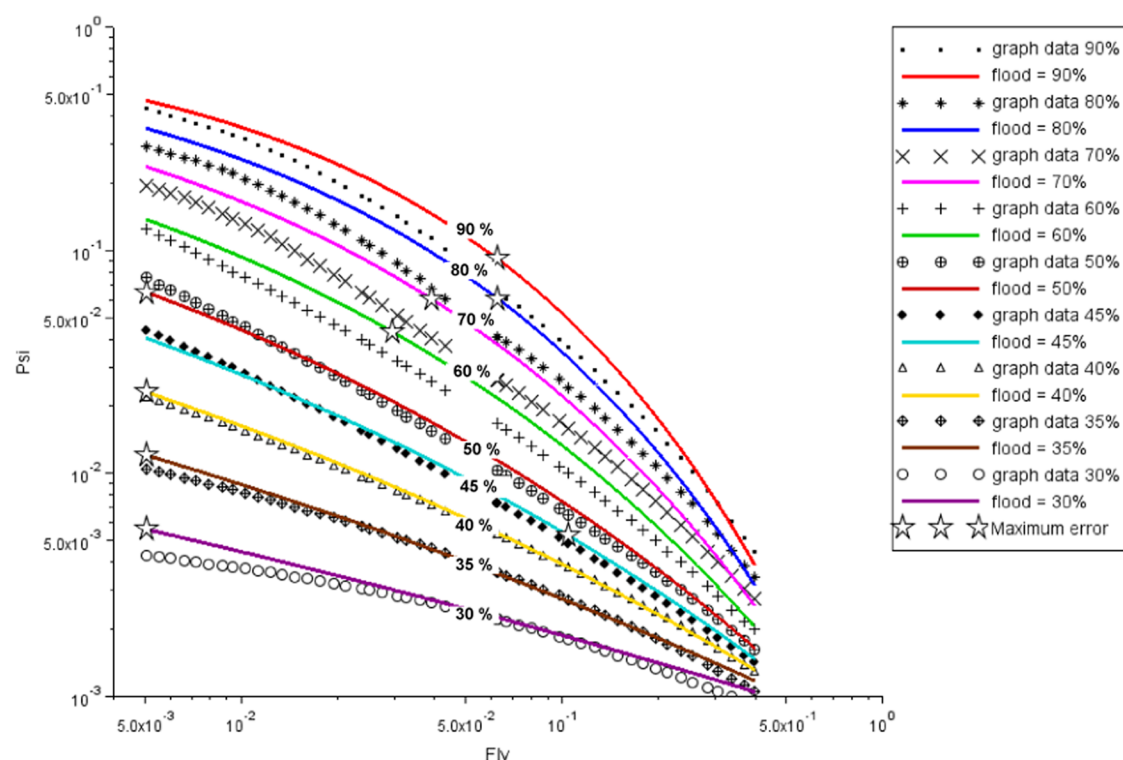


Figure 6. Comparison of the original data of entrainment fraction with the correlation proposed by Economopoulos.<sup>8</sup>

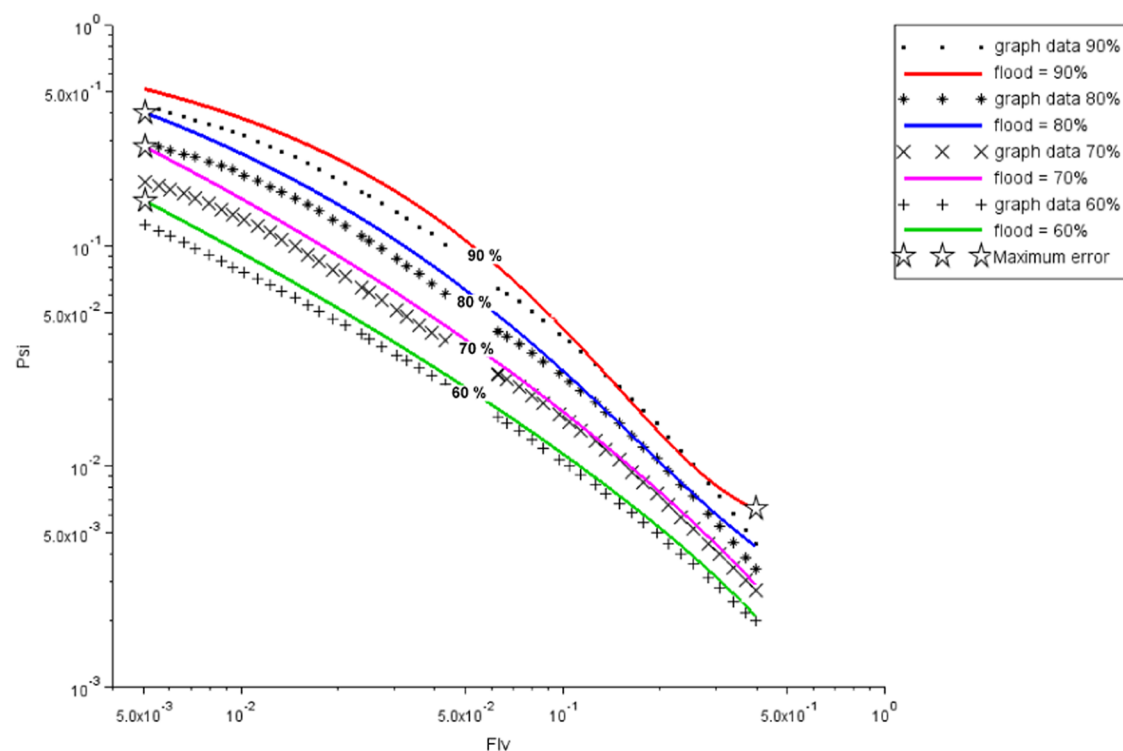


Figure 7. Comparison of the original data of entrainment fraction with the correlation proposed by Lygeros and Magoulas.<sup>9</sup>

The analysis of the performance of each correlation does not indicate conclusively what is the most accurate alternative. The lowest average errors related to different values of fractional flooding are associated with different correlations (e.g., the lowest average error for the values of fractional flooding 35%, 40%, and 60% are associated with the correlations of

Economopoulos,<sup>8</sup> Lygeros and Magoulas,<sup>9</sup> and Ogboja and Kuye,<sup>11</sup> respectively).

The maximum errors associated with the correlations of Ogboja and Kuye<sup>11</sup> and Lygeros and Magoulas<sup>9</sup> are located at the lowest or the highest values of Flv. The maximum errors of the correlation Economopoulos<sup>8</sup> are located at the lowest or intermediate values of Flv.

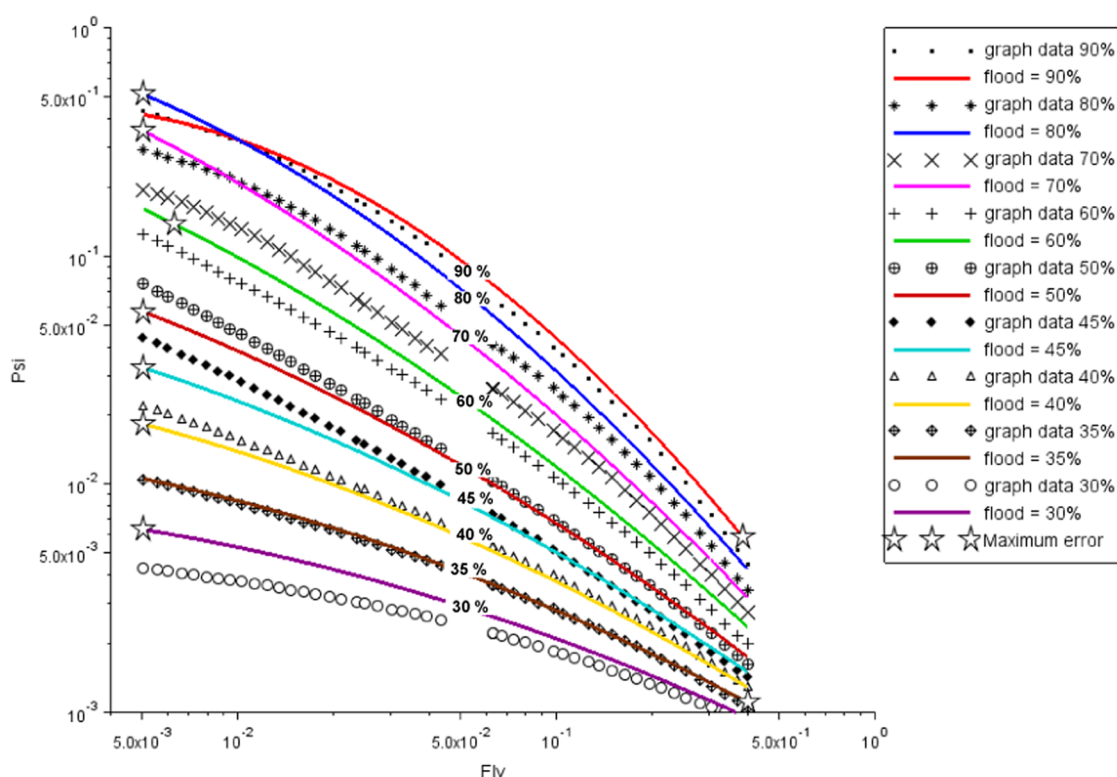


Figure 8. Comparison of the original data of entrainment fraction with the correlation proposed by Ogboja and Kuye.<sup>11</sup>

Table 14. New Parameters for the Correlation of Economopoulos,<sup>8</sup> Considering Two Regions

Tray spacing (in)	Flv	$\theta_{C_{sb}1}$	$\theta_{C_{sb}2}$	$\theta_{C_{sb}3}$	$\theta_{C_{sb}4}$	$\theta_{C_{sb}5}$	$\theta_{C_{sb}6}$
6	$\leq 0.1263$	4.4000697	-0.5775733	4.8304139	2.6799314	4.4557714	-3.103613
9		4.7269972	-0.3699619	-4.999006	-0.5977399	-4.9983493	0.8334274
12		4.7459131	-0.2593782	-4.3885062	-0.4428965	-5.9949766	1.2393609
18		4.9470236	-0.1610794	-4.9915123	-0.2783693	-4.9998887	1.0445176
24		4.9999759	-0.1093138	-4.1404762	-0.1918679	-4.9961433	1.2133206
36		4.1266714	3.1289251	-3.6024925	-0.1147729	-4.6425641	0.9738661
6	$> 0.1263$	4.5178369	-0.5942546	4.8414634	-0.9702420	4.6445794	-2.557437
9		3.7605707	-0.3571457	4.6764574	-0.6410964	4.8750665	-3.0671162
12		4.3937897	4.667488	4.9192652	-0.4728603	4.7185437	-3.1293533
18		3.0470916	3.5050506	4.9563515	-0.3076338	4.9621191	-3.6316262
24		3.3388334	3.2393369	4.7410224	-0.2191914	4.797542	-3.8619151
36		3.8511541	3.7137044	4.6400848	-0.1383541	4.6007155	-3.6763634

**2.3. Critical Analysis.** The investigated correlations present different performances, from good adherence to the original data to very poor fittings. The main question to be made is if these errors are tolerable, that is, if the design solutions obtained using these correlations would later violate the operational limits established. Additionally, considering optimization design problems, there is also the issue of whether the use of incorrect correlations leads to suboptimal designs.

In the rest of our paper, we recalculate the parameters of the above-presented correlations. In addition, we study situations in the design procedure where the correlation predictions indicate the acceptance of a distillation column that is, in reality, infeasible (i.e., a “false positive” result) and other situations where the correlation indicates that a certain distillation column is infeasible, but it is feasible after all (i.e., a “false negative”).

### 3. PARAMETER ESTIMATION PROCEDURE

The previous section showed that the errors associated with the correlations available in the literature for the evaluation of flooding and entrainment can be significant. Therefore, aiming at reducing these errors, we applied a parameter estimation procedure to reevaluate the correlations’ parameters.

The objective function employed for the estimation of the parameters was the weighted least-squares:

$$F_{obj} = \min_{\theta} \sum_{i=1}^{NP} \frac{(y_i^{graph}(\mathbf{x}_i) - y_i^{model}(\mathbf{x}_i, \theta))^2}{\sigma_{y,i}^2} \quad (15)$$

where  $i$  is the index of each data point collected from the Fair’s graphs ( $i = 1, \dots, NP$ ),  $\mathbf{x}_i$  is the vector of the independent variable values at the data point  $i$ ,  $\theta$  is the vector of parameters to be estimated,  $y_i^{graph}(\mathbf{x}_i)$  is the data obtained from the Fair’s graph ( $C_{sb}$  or  $\psi$ ) for each set of independent variables  $\mathbf{x}_i$  (Flv and  $l$  or only Flv for flooding correlations, Flv and Fflood or only Flv for

the entrainment correlations), and  $y_i^{\text{model}}(x_i, \theta)$  is the correlation prediction of the corresponding dependent variable associated with the set of independent variables  $x_i$  and parameters  $\theta$ , and  $\sigma_{y,i}^2$  is the variance of the data points. The values of the variance of the data points are unknown, but we use  $\sigma_{y,i}^2$  to avoid a bias of the model output toward larger values of the dependent variables. Therefore, the value adopted for  $\sigma_{y,i}^2$  is  $0.1y_i^{\text{graph}}(x_i)$ . This aspect is particularly important due to the large variations of the values of  $C_{sb}$  and  $\psi$  in the data set collected from the Fair's graphs.

#### 4. PARAMETER ESTIMATION RESULTS

The estimation of the parameters for the correlations of flooding and entrainment was conducted without any linearization

**Table 15. Error of the Flooding Correlation by Economopoulos<sup>8</sup> with New Parameters, Considering Two Regions**

Tray spacing (in)	Average error (%)	Maximum error (%)
6	1.46	6.67
9	1.45	7.89
12	1.41	4.64
18	1.21	5.17
24	1.38	11.16
36	0.91	4.11

procedure previously applied to the models. The parameter estimation procedures employed global optimization solvers initialized by the solutions obtained by local solvers using the GAMS software (version 24.7.1). The unique exception was the parameter estimation of the flooding correlation using the Economopoulos<sup>8</sup> correlation. In this case, the GAMS solvers

failed, then the initialization was provided by a stochastic algorithm, and the parameter estimation problem was solved using a local solver from Scilab. The computational details of the numerical solution of the parameter estimation problems are depicted in the Supporting Information (Section S2), including the description of the solvers employed and the time required to solve each instance. The initial estimates employed in the parameter estimation problems were the corresponding values of the correlation parameters presented in the literature.

Aiming at providing additional error reductions of the correlation predictions, parameter estimations were also tried using the split of the domain. For each region, a different set of parameters were obtained. The corresponding results are shown below. Equivalent results without the domain split of the parameter estimation are available in the Supporting Information (Sections S3 and S4).

**4.1. Flooding Correlation.** In the flooding correlation, the parameters of the models of Economopoulos,<sup>8</sup> Lygeros and Magoulas,<sup>9</sup> Ogboja and Kuye,<sup>11</sup> and Kessler and Wankat<sup>10</sup> were determined.

The Flv domain was split into two regions, limited by the median of the set of Flv values (one set is limited by  $\text{Flv} \leq 0.1263$  and another is defined by  $\text{Flv} > 0.1263$ ), followed by the application of the parameter estimation procedure to each region separately (i.e., two sets of parameters were evaluated, each one valid for a given region).

**4.1.1. Economopoulos.** The parameters were determined for each discrete value of the tray spacing present in Fair's data, considering the split of the Flv range in two regions.<sup>8</sup> The Simplex optimization method<sup>28,29</sup> was used with initial estimates provided by the Particle Swarm Optimization (PSO).<sup>30</sup> Because of the stochastic nature of PSO, 10 parameter estimation runs

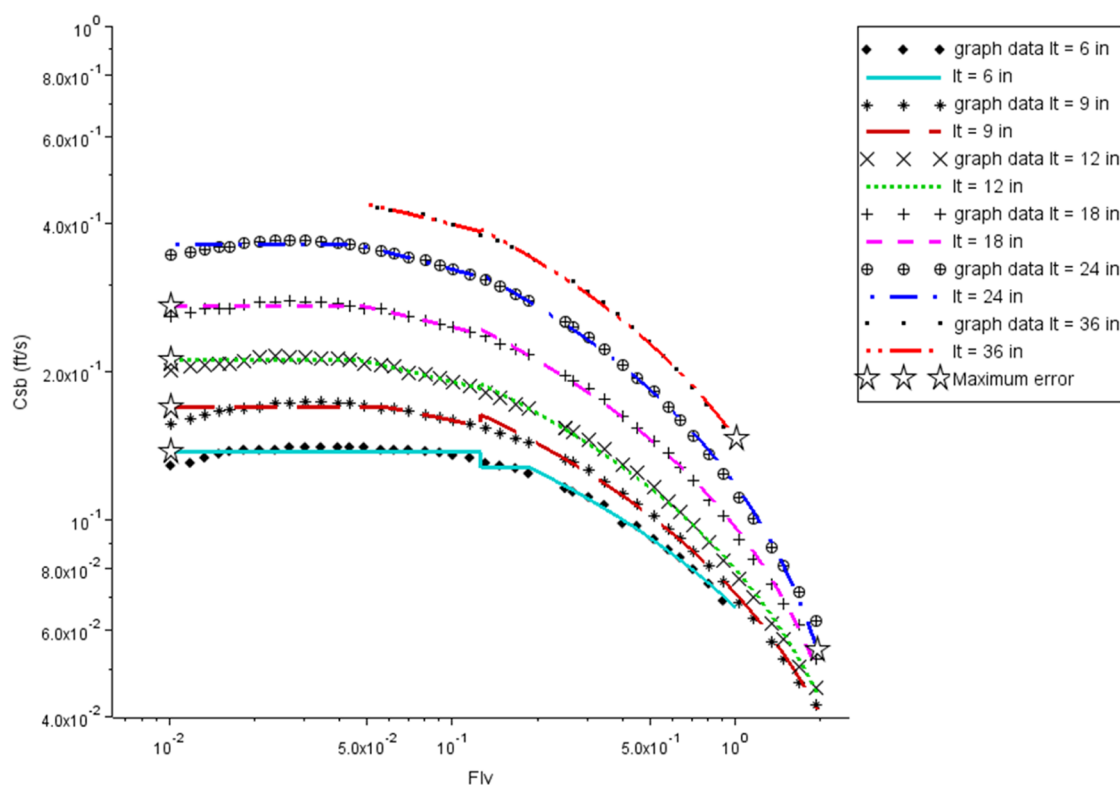


**Figure 9.** Comparison of Fair's data for the Souders–Brown constant with the correlation proposed by Economopoulos<sup>8</sup> with new parameters, considering two regions.



**Table 16.** New Parameters for the Correlation of Lygeros and Magoulas,<sup>9</sup> Considering Two Regions

Tray spacing (m)	Flv	$\theta_{C_{sb}1}$	$\theta_{C_{sb}2}$	$\theta_{C_{sb}3}$	$\theta_{C_{sb}4}$	$\theta_{C_{sb}5}$
0.1524	$\leq 0.1263$	-83.6202	9.02113252	-1.18390552	2.02951064	5.47697064
0.2286		0.04761459	0.70987588	3.51949019	$2.591576 \times 10^{+6}$	6.18532635
0.3048		0.05633279	0.59564551	3.62416469	$1.367922 \times 10^{+4}$	3.92480287
0.4572		0.07300709	0.56207926	5.14476362	$2.253357 \times 10^{+4}$	4.09383704
0.6096		0.09482061	0.83479308	8.02227176	$1.022961 \times 10^{+4}$	3.78047576
0.9144	$> 0.1263$	0.14942903	-0.00867470	0.63306988	-5.75281342	0.67489572
0.1524		0.00976870	0.15259236	0.75500000	1.29662151	0.92188085
0.2286		0.00514023	0.16754077	0.75499476	1.21933126	0.73465549
0.3048		0.00701328	0.15604655	0.75500000	1.34131675	0.77460268
0.4572		0.00567572	0.17037018	0.75500000	1.40632291	0.67788468
0.6096		0.00771888	0.17865301	0.75500000	1.50815571	0.69988173
0.9144		-0.01764594	$1.979101 \times 10^{-7}$	$-1.54346 \times 10^{+2}$	-1.17643579	0.53675751

**Table 17.** Errors of the Flooding Correlation by Lygeros and Magoulas<sup>9</sup> with New Parameters, Considering Two Regions

Tray spacing (m)	Average error (%)	Maximum error (%)
0.1524	0.99	7.05
0.2286	0.89	7.82
0.3048	0.71	4.66
0.4572	0.74	5.19
0.6096	0.77	4.84
0.9144	0.25	0.94

were made, and the one with the lowest objective function is presented here.

The results are listed in Table 14. Table 15 shows the errors of the correlation with the new values of the parameters, and Figure 9 shows the corresponding comparison between the original data and the correlation. In some cases, there is a discontinuity in the prediction of the correlation in the boundary between the two regions. Because the insertion of a constraint in the parameter estimation problem to eliminate this discontinuity compromised the accuracy of the predictions, we preferred to

keep the results where the parameter estimations in both regions were applied independently.

**4.1.2. Lygeros and Magoulas.<sup>9</sup>** The parameters were determined for each discrete value of the tray spacing present in Fair's data using the ANTIGONE solver<sup>25</sup> with initial estimates provided by a previous CONOPT solver run.<sup>26</sup>

Table 16 shows the new parameters. The errors of the correlation with the new parameters are listed in Table 17. Figure 10 shows the corresponding comparison between the original data and the correlation.

**4.1.3. Ogboja and Kuye.<sup>11</sup>** New parameters were determined for each discrete value of the tray spacing for the Ogboja and Kuye.<sup>11</sup> The parameter estimation problem was solved using the BARON solver<sup>27</sup> associated with the CONOPT solver<sup>26</sup> to provide an initial estimate.

Table 18 shows the new parameters considering the split of the Flv range in two regions. The errors of the correlation with the new parameters are shown in Table 19, and Figure 11 shows the corresponding comparison between the original data and the correlation.

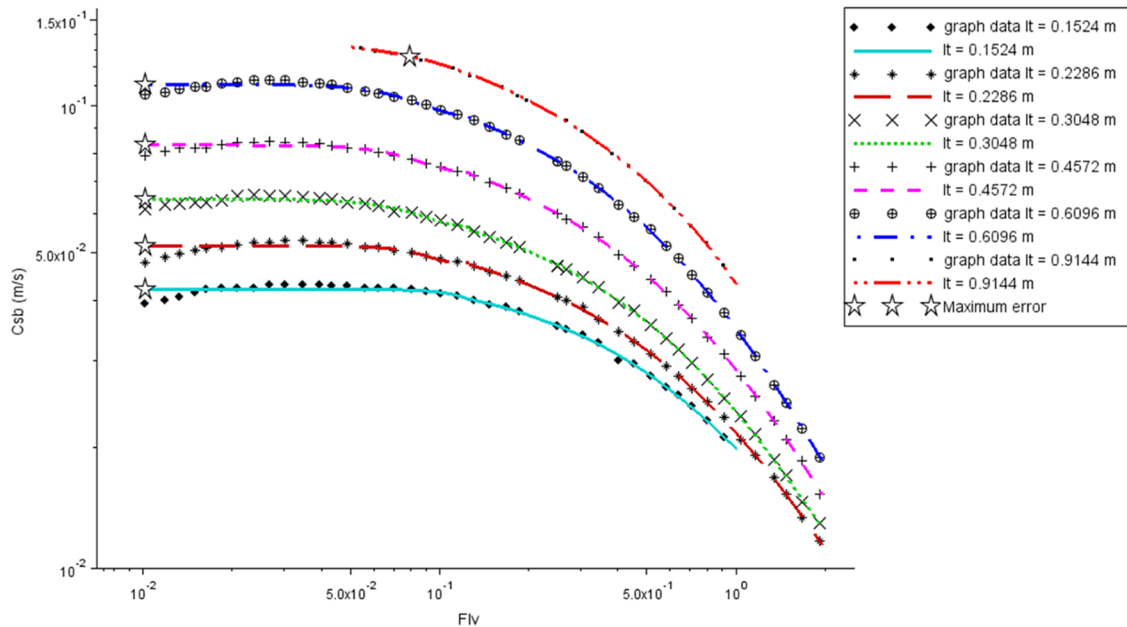


**Figure 10.** Comparison of Fair's data for the Souders–Brown constant with the correlation proposed by Lygeros and Magoulas<sup>9</sup> with new parameters, considering two regions.

Table 18. New Parameters for the Correlation of Ogboja and Kuye,<sup>11</sup> Considering Two Regions

Tray spacing (m)	Flv	$\theta_{C_{sb},1}$	$\theta_{C_{sb},2}$	$\theta_{C_{sb},3}$	$\theta_{C_{sb},4}$	$\theta_{C_{sb},5}$	$\theta_{C_{sb},6}$
0.1524	$\leq 0.1263$	-0.4168	3.0206	-0.3346	1.9667	3.0713	-20.0825
0.2286		0.0525	0	-0.0461	0	0.0138	0
0.3048		0.7902	-2.3816	-0.2686	0.6759	-1.2452	4.1504
0.4572		-1.2979	3.0206	-0.9831	1.9667	-0.3059	0.7279
0.6096		0.1098	0	-0.1174	0	0.03841	0
0.9144		-2.6236	3.0206	-1.9837	1.9667	3.0713	-3.2559
0.1524	$> 0.1263$	0.0129	0.2011	0.0061	-0.2686	-0.008	0.1229
0.2286		0.0129	0.1731	0.0153	-0.2686	-0.008	0.0954
0.3048		0.0129	0.1688	0.0193	-0.2686	-0.008	0.0914
0.4572		0.0129	0.1535	0.0388	-0.2686	-0.008	0.0763
0.6096		0.0129	0.1589	0.0464	-0.2686	-0.008	0.0761
0.9144		0.0129	0.1373	0.0603	-0.2686	-0.008	0.1116

Table 19. Error of the Flooding Correlation by Ogboja and Kuye<sup>11</sup> with New Parameters, Considering Two Regions

Tray spacing (m)	Average error (%)	Maximum error (%)
0.1524	1.94	9.88
0.2286	3.20	18.81
0.3048	4.16	29.10
0.4572	4.55	37.23
0.6096	5.46	43.77
0.9144	2.01	10.38

Table 20. New Parameters of the Quadratic Correlation of Kessler and Wankat,<sup>10</sup> Considering Two Regions

Tray spacing (in)	Flv	$\theta_{C_{sb},1}$	$\theta_{C_{sb},2}$	$\theta_{C_{sb},3}$
6	$\leq 0.1263$	1.0605	0.2969	0.1054
9		1.0973	0.4533	0.1533
12		1.0454	0.4795	0.1528
18		0.9432	0.4925	0.1576
24		0.8635	0.5450	0.1729
36		0.8152	0.6473	0.2313
6	$> 0.1263$	1.1837	0.5868	0.2814
9		1.1563	0.6597	0.3127
12		1.1110	0.7059	0.3320
18		1.0270	0.7434	0.3360
24		0.9423	0.7964	0.3596
36		0.8393	0.7543	0.3245

4.1.4. *Kessler and Wankat.*<sup>10</sup> New parameters were estimated for the Kessler and Wankat<sup>10</sup> correlation for each discrete value of the tray spacing. Only the quadratic equation was employed because it is simpler and provides a good fit. The parameter estimation problem was solved using the BARON solver<sup>27</sup> associated with the CONOPT solver<sup>26</sup> to provide an initial estimate.

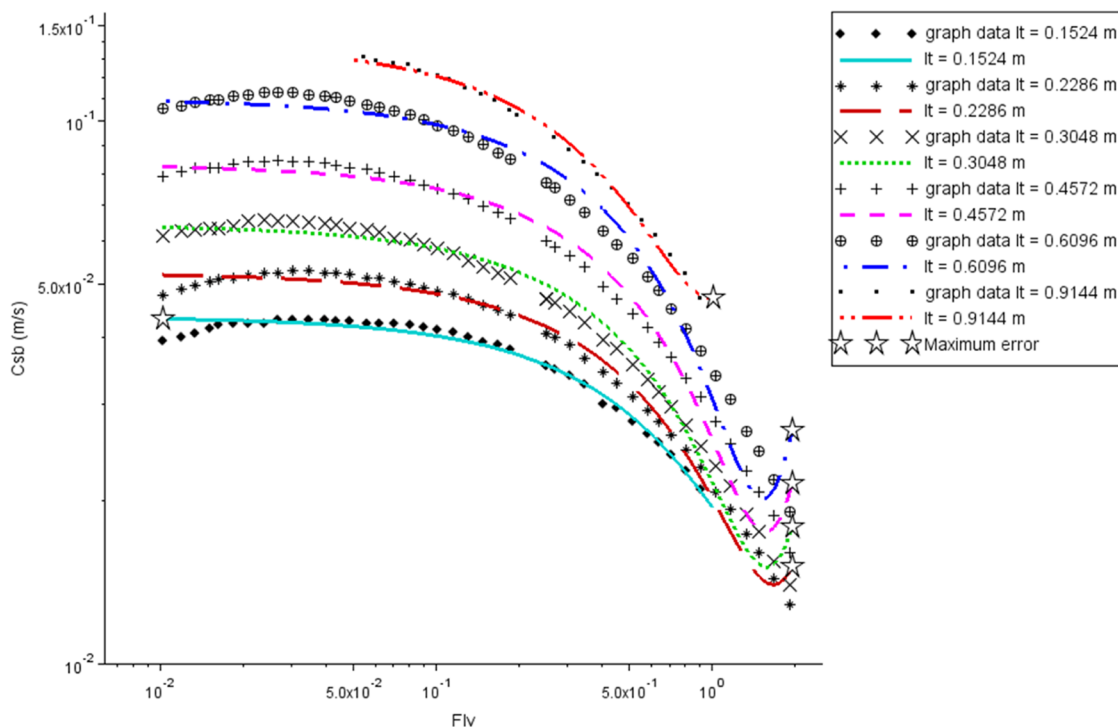


Figure 11. Comparison of Fair's data for the Souders–Brown constant with the correlation proposed by Ogboja and Kuye<sup>11</sup> with new parameters, considering two regions.

**Table 21. Errors of the Flooding Quadratic Correlation by Kessler and Wankat<sup>10</sup> with New Parameters, Considering Two Regions**

Tray spacing (in)	Average error (%)	Maximum error (%)
6	0.46	2.47
9	0.44	2.07
12	0.45	2.48
18	0.50	4.27
24	0.52	1.82
36	0.45	2.81

Table 20 shows the new parameters after splitting Flv into two regions, Table 21 shows the errors of the correlation with new parameters for each region, and Figure 12 shows a comparison between the original data and the correlation predictions.

**4.1.5. Performance Comparison.** Table 22 shows a comparison of the accuracy of the flooding correlations with the original parameters (Tables 4 and 8) and with the parameters obtained in this article (Tables 15, 17, 19, and 21) for different values of tray spacing. According to these data, there is a considerable reduction in the average and maximum errors (e.g., the upper bounds of the average and maximum error ranges were reduced by more than a half).

**4.2. Entrainment Correlation.** The parameters of the correlations of Economopoulos,<sup>8</sup> Lygeros and Magoulas,<sup>9</sup> and Ogboja and Kuye<sup>11</sup> were reevaluated using the parameter estimation procedure discussed in the previous section. Considering the reduction of the error shown above through the splitting of the correlation domain, the same procedure was applied here. Instead of using a single set of parameters for the entire domain of the independent variables, the domain was split

into a certain number of regions, and the parameter estimation was applied for each region. Aiming at attaining a satisfactory error reduction, more than two regions were necessary for the parameter estimation involving the entrainment correlations of Lygeros and Magoulas<sup>9</sup> and Ogboja and Kuye<sup>11</sup>

**4.2.1. Economopoulos.**<sup>8</sup> The parameter estimation of the Economopoulos<sup>8</sup> correlation model was done by splitting the domain of Flv and Fflood into 6 regions. The definition of the number of regions and the limits of each region was established through successive trials until a satisfactory error reduction was attained. The parameter estimation problem was solved using the ANTIGONE solver<sup>25</sup> with initial estimates provided by a previous CONOPT solver run.<sup>26</sup> The results are displayed in Table 23. Table 24 shows the errors in the correlation with new parameters. Figure 13 shows the comparison between the Fair's data and the correlation with new parameters.

**4.2.2. Lygeros and Magoulas.**<sup>9</sup> The parameter estimation of the Lygeros and Magoulas<sup>9</sup> correlation was done for each discrete value of the flooding fraction present in Fair's graph using the solver CONOPT.<sup>26</sup>

The estimated parameters are listed in Table 25. Table 26 shows the errors of the correlation with the new parameters, and Figure 14 shows the comparison between the Fair's data and the correlation prediction.

**4.2.3. Ogboja and Kuye.**<sup>11</sup> The parameter estimation of the correlation of Ogboja and Kuye<sup>11</sup> was done by splitting the domain of Flv and Fflood into 3 regions using the solver CONOPT.<sup>26</sup> The definition of the number of regions and the limits of each region were established through successive trials until a satisfactory error reduction was attained. The results are displayed in Table 27. Table 28 shows the errors and the corresponding maximum error of the correlation with the new

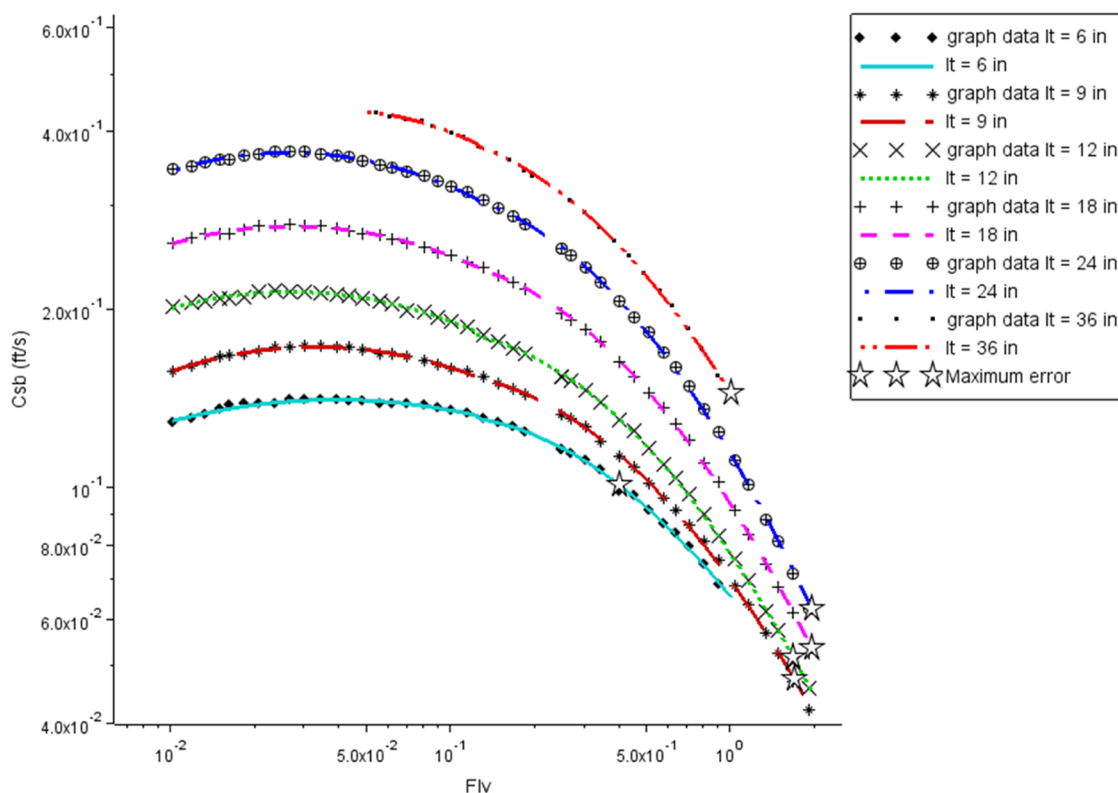


**Figure 12.** Comparison of Fair's data for the Souders–Brown constant with the quadratic correlation proposed by Kessler and Wankat<sup>10</sup> with new parameters, considering two regions.

**Table 22. Performance Comparison of the Entrainment Correlations with the Original Parameter and the New Ones**

Correlation	Original parameters		Parameters from this paper	
	Average error range (%)	Maximum error range (%)	Average error range (%)	Maximum error range (%)
Economopoulos <sup>8</sup>	4.32–52.33	15.76–85.06	0.91–1.46	4.11–11.16
Lygeros and Magoulas <sup>9</sup>	2.51–5.05	4.57–21.52	0.25–0.99	0.94–7.82
Ogboja and Kuye <sup>11</sup>	10.76–17.40	15.17–504.05	1.94–5.46	9.88–43.77
Kessler and Wankat <sup>10</sup>	1.24–5.53	7.47–14.81	0.44–0.52	1.82–4.27

**Table 23. New Parameters of the Correlation of Economopoulos<sup>8</sup> for Evaluation of the Fractional Entrainment**

Flv	Fflood	$\theta_{\psi,1}$	$\theta_{\psi,2}$	$\theta_{\psi,3}$	$\theta_{\psi,4}$
Flv $\leq$ 0.05	Fflood $\geq$ 0.6	3.377	8.327	−0.211	0.773
0.05 < Flv $\leq$ 0.1	Fflood $\geq$ 0.6	3.896	4.551	−0.273	0.734
Flv > 0.1	Fflood $\geq$ 0.6	7.758	−0.175	−0.062	0.478
Flv $\leq$ 0.05	Fflood < 0.6	3.862	9.567	−0.233	0.916
0.05 < Flv $\leq$ 0.1	Fflood < 0.6	7.028	1.145	−0.098	0.563
Flv > 0.1	Fflood < 0.6	7.434	0.267	−0.071	0.503

**Table 24. Errors of Entrainment Correlations by Economopoulos<sup>8</sup> with New Parameters, Considering Multiple Regions**

Fflood (%)	Average error (%)	Maximum error (%)
90	1.95	7.91
80	1.56	7.10
70	2.01	7.23
60	2.72	11.40
50	1.26	4.08
45	1.42	3.75
40	2.72	5.25
35	2.96	4.92
30	3.85	8.24

parameters. Figure 15 shows the comparison between Fair's data and the correlation prediction.

**4.2.4. Performance Comparison.** Table 29 shows a comparison of the accuracy of the entrainment correlations with the original parameters (Tables 9–11) and with the parameters obtained in this paper (Tables 23, 25, and 27) for different fractional flooding. It is possible to observe that a large improvement in the model predictions was attained.

## 5. PERFORMANCE OF THE CORRELATIONS

This paper has shown that the correlations available in the literature for sieve tray performance may present considerable deviations from the original Fair's data, and the application of a new procedure for parameter estimation can reduce these errors significantly.

Therefore, considering that the original correlations were employed in several other papers, this section presents an analysis of how the corresponding deviations can affect the design of a distillation column, comparing the design solutions obtained by using these correlations with the design solutions by using the improved predictions developed in this paper.

Three design optimization problems of the distillation columns were considered. Example 1 is the design of a depropanizer column and was taken from Kister,<sup>2</sup> with larger flow rates (the original values of the flow rates were multiplied by 2.0). Example 2 is the design of a distillation column for acetone recovery from a waste stream and was taken from Towler and Sinnott,<sup>3</sup> also with larger flow rates (the original values were multiplied by 2.0). Example 3 consists of a methanol purification

column and was taken from Kiss and Ignat,<sup>31</sup> with lower flow rates (the original values were multiplied by 0.5). The proposed modifications of the original flow rates were applied to generate a data set with high and low throughputs, therefore providing a clearer assessment of the accuracy of the correlations. The optimization search space and the details of each example are described in the Supporting Information (Section S5).

The distillation column of each example was optimally designed using the Set Trimming procedure described by Costa and Bagajewicz,<sup>32</sup> applied to a sieve tray design.<sup>33</sup> This procedure guarantees the global optimality of the design problem and is robust.

The design problems were solved using three different alternatives of correlations: (1) Correlations of Economopoulos<sup>8</sup> for flooding and entrainment using the parameter values from the literature; (2) correlations of Ogboja and Kuye<sup>11</sup> for flooding and entrainment using the parameter values from the literature; and (3) correlations of Kessler and Wankat<sup>10</sup> for flooding and Ogboja and Kuye<sup>11</sup> for entrainment using the new values of the parameters developed in this paper. The optimal design solutions are depicted in Table 30. The geometric details of each optimal solution are described in the Supporting Information (Section S5).

The results displayed in Table 30 indicate deviations among the different design results. In Example 1, the original literature correlations are associated with distillation columns with smaller diameters. However, considering that the correlations with the new parameters proposed in this work provide the most accurate predictions, the distillation columns designed with the original correlations may not operate adequately. The opposite situation occurs in Example 3, where the distillation columns designed with the original correlations are associated with a larger diameter, i.e., the literature correlations lead to the exclusion of the search for a feasible distillation column associated with a smaller capital cost. The results of Example 2 contain both problems: one column based on the literature values of the correlations parameters has a smaller diameter than the alternative designed with the updated set of parameter values, and the other column obtained using literature values of the parameters has a higher diameter than the alternative designed using the proposed set of parameter values.

Aiming at providing a better comprehension of the detachments indicated in Table 30, the analysis of the correlations was also conducted through the evaluation of each solution

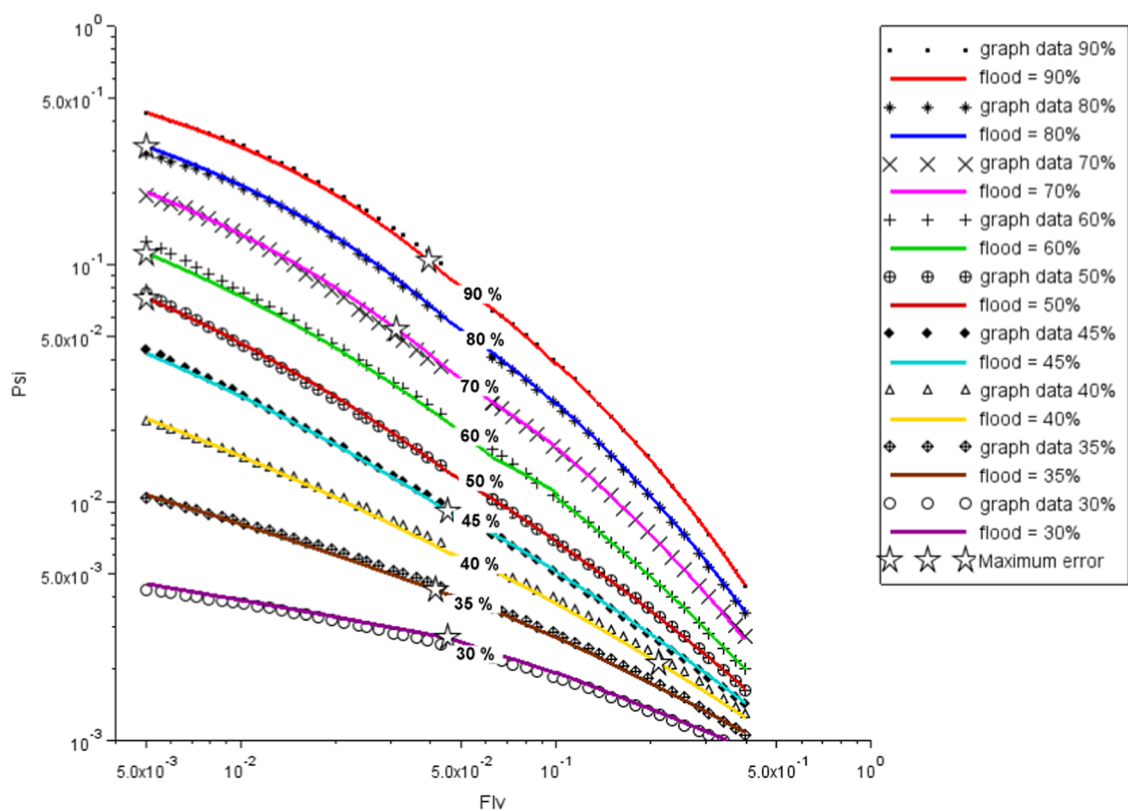


**Figure 13.** Comparison of Fair's data for the entrainment fraction with the correlation proposed by Economopoulos<sup>8</sup> with new parameters, considering multiple regions.

**Table 25.** New Parameters of the Correlation of Lygeros and Magoulas<sup>9</sup> for Evaluation of the Fractional Entrainment for Each Flood Value

Fflood (%)	$\theta_{\psi,1}$	$\theta_{\psi,2}$	$\theta_{\psi,3}$	$\theta_{\psi,4}$
90	$3.178 \times 10^{-3}$	1.262	-9.116	0.4071
80	$2.067 \times 10^{-3}$	1.381	-8.794	0.3322
70	$4.499 \times 10^{-4}$	4.741	-9.054	0.2003
60	$-6.575 \times 10^{-4}$	23.761	-10.264	0.1270
50	$-2.475 \times 10^{-4}$	531.301	-13.484	0.0794
45	$-1.377 \times 10^{-4}$	38.812	-11.025	0.0919
40	$-4.035 \times 10^{-4}$	6.598	-8.946	0.0857
35	$-3.152 \times 10^{-4}$	0.0742	-4.658	0.1666
30	$2.677 \times 10^{-4}$	0.0066	-3.242	0.3532

**Table 26.** Errors of Entrainment Correlations by Lygeros and Magoulas<sup>9</sup> with New Parameters for Each Fflood Value

Fflood (%)	Average error (%)	Maximum error (%)
90	2.35	25.01
80	3.01	22.32
70	2.72	9.10
60	0.24	3.40
50	0.36	2.77
45	0.19	1.02
40	0.26	1.61
35	0.18	0.56
30	0.23	1.22

candidate of the search space of the design problem. This analysis is based on 783,900 sets of values of different tray dimensions.

Considering the constraints of flooding (eq 1) and entrainment (eq 10), the results are classified into four different classes based on the comparison of the tray alternatives that did or did not abide by the restrictions of flooding and entrainment. This analysis considers that the set of parameters presented in this work is associated with the most accurate predictions, as shown in the results above. Therefore, each design solution based on the literature correlation parameters can be classified according to its deviation from the corresponding results attained using the updated values of the parameters presented here as follows:

- Feasible: the tray dimensions are feasible using the predictions based on the literature parameters and also using the parameter values developed in this paper.
- Infeasible: the tray dimensions are infeasible using the predictions based on the literature parameters and also using the parameter values developed in this paper.



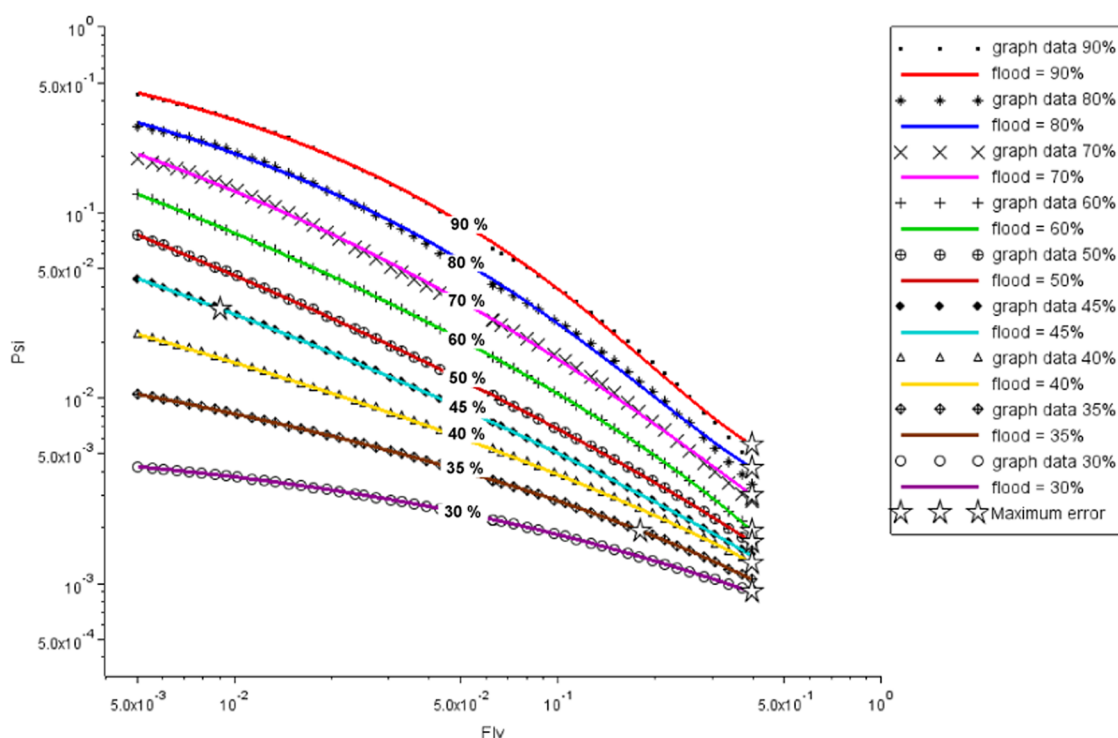


**Figure 14.** Comparison of the experimental data for entrainment fraction with the correlation proposed by Lygeros and Magoulas<sup>9</sup> with new parameters.

**Table 27.** New Parameters of the Correlation of Ogboja and Kuye<sup>11</sup> for Evaluation of the Fractional Entrainment, Considering Multiple Regions

Flv	Fflood	$\theta_{\psi,1}$	$\theta_{\psi,2}$	$\theta_{\psi,3}$	$\theta_{\psi,4}$	$\theta_{\psi,5}$	$\theta_{\psi,6}$	$\theta_{\psi,7}$	$\theta_{\psi,8}$
Flv $\leq 0.15$	Fflood $\geq 0.5$	-7.395	0.324	-0.222	2.516	0.146	-0.430	0.234	-0.153
Flv $> 0.15$	Fflood $\geq 0.5$	-7.743	0.270	-0.170	3.001	0.927	-3.806	4.706	-2.217
$\forall$ Flv	Fflood $< 0.5$	-7.903	1.135	0.073	2.066	-0.647	4.309	-10.301	8.308

**Table 28.** Errors of the Entrainment Correlations of Ogboja and Kuye<sup>11</sup> with New Parameters, Considering Multiple Regions

Fflood (%)	Average error (%)	Maximum error (%)
90	1.17	4.58
80	1.56	4.84
70	2.54	6.09
60	0.69	3.94
50	1.51	3.57
45	1.64	5.62
40	2.03	4.25
35	1.59	4.78
30	2.69	4.44

- False positive: the correlation of the literature indicates that the design is feasible, but the prediction developed in this paper indicates that the design is not feasible.
- False negative: the correlation of the literature indicates that the design is infeasible, but the prediction developed in this paper indicates that the design is feasible.

The feasible and infeasible cases correspond to results where the deviations between the correlations using the literature parameters and the updated values of the correlations do not affect the design. However, false positive and false negative cases indicate that the accuracy limitations associated with the original correlations affect the column design.

The main deviations are associated with the design problem of Example 1, as discussed below. The comparison of the performance of the correlations of Economopoulos<sup>8</sup> with our predictions is shown in Figure 16. False positives are associated with the flooding constraint, and false negatives are associated with the entrainment constraint, as shown in Figure 16a,b, respectively. These deviations are relevant because they affect the solution of the optimal design problem, as shown in Table 30. The solution to the optimal design problem using the correlation of Economopoulos<sup>8</sup> is a distillation column with a cost of \$316,361.07. However, this solution is a false positive, i.e., testing this optimal design with the more accurate predictions developed in this paper, it is verified that this column is not feasible.

The correlation of Ogboja and Kuye<sup>11</sup> presents a smaller number of false positives and negatives, as depicted in Figure 17. However, these deviations also affect the solution of the optimal design problem, i.e., another false positive is associated with the design optimization.

Similar analyses are available in the Supporting Information for Examples 2 and 3 (Section S5). The number of deviations is smaller, but as shown in Table 30, they can affect the result of the optimal design.

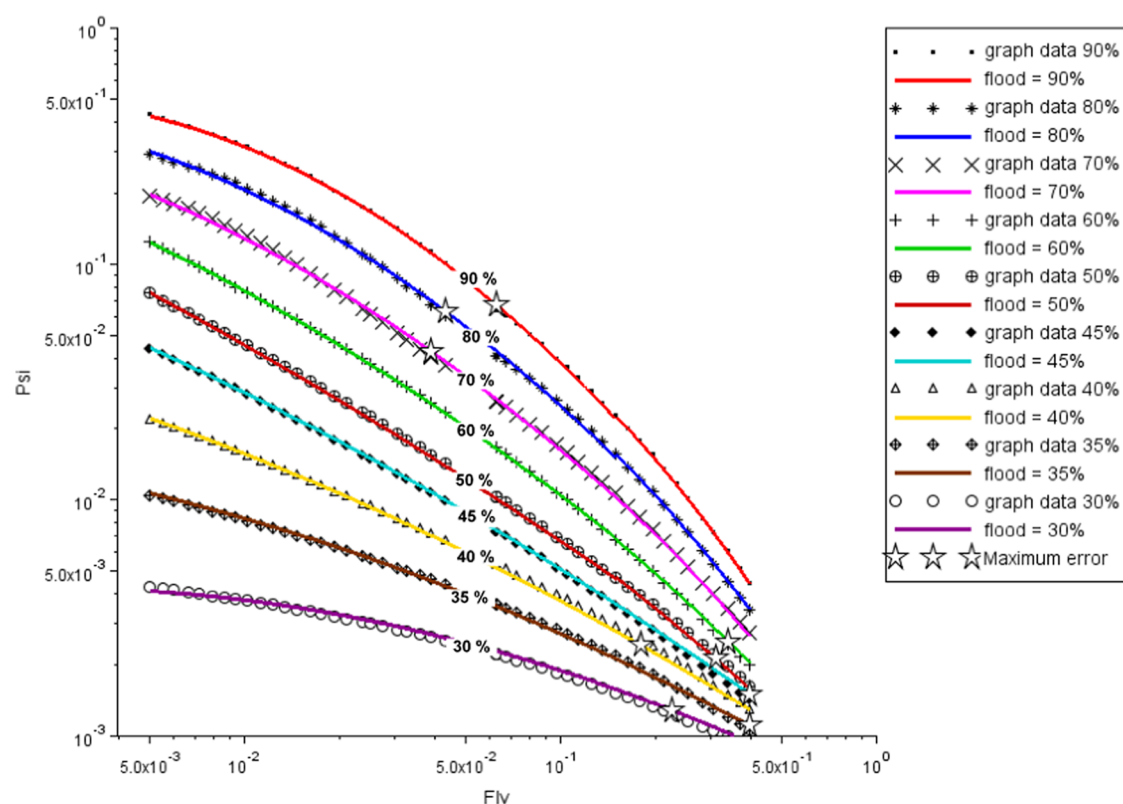


Figure 15. Comparison of the original data for the entrainment fraction with the correlation proposed by Ogboja and Kuye<sup>11</sup> with new parameters.

Table 29. Performance Comparison of the Entrainment Correlations with the Original Parameter and the New Ones

Correlation	Original parameters		Parameters from this paper	
	Average error range (%)	Maximum error range (%)	Average error range (%)	Maximum error range (%)
Economopoulos <sup>8</sup>	2.95–28.94	5.79–50.60	1.26–3.85	3.75–11.40
Lygeros and Magoulas <sup>9</sup>	12.88–15.26	27.52–44.68	0.18–3.01	0.56–25.01
Ogboja and Kuye <sup>11</sup>	1.54–36.24	4.73–82.41	0.69–2.69	3.57–6.09

Table 30. Design Results

Example	Result	Economopoulos <sup>8</sup>	Ogboja and Kuye <sup>11</sup>	New correlations parameters
1	Cost total (\$)	316,361.07	352,484.38	441,644.54
	Column diameter (m)	3.0480	3.3528	4.064
	Tray spacing (m)	0.9144	0.9144	0.9144
2	Cost total (\$)	36,738.14	45,604.67	40,852.56
	Column diameter (m)	0.9144	1.2700	1.2700
	Tray spacing (m)	0.9144	0.6096	0.4572
3	Cost total (\$)	31,955.10	31,955.10	30,643.87
	Column diameter (m)	0.7620	0.7620	0.6096
	Tray spacing (m)	0.4572	0.4572	0.6096

## 6. CONCLUSIONS

This paper presents an update of the flooding and entrainment correlation parameters from the literature for sieve trays. First, the errors in the literature correlations compared to those in the original data were analyzed. Usually, the maximum errors are located at the beginning or end of the range of the original data. To reduce errors and improve the fit of the curves, several attempts were made, and the best parameter updates obtained were with the flooding correlation of Kessler and Wankat<sup>10</sup> and the entrainment correlation of Ogboja and Kuye.<sup>11</sup>

The readjustment of correlations was applied in three examples from the literature on globally optimal design

procedures, and the result was compared with the literature correlations Economopoulos<sup>8</sup> and Ogboja and Kuye.<sup>11</sup> In all three examples, the optimal tray found is a false positive or a false negative; thus, they are infeasible results for our readjustment (false positive) or results that eliminate feasible designs that should be considered at lower cost (false negative).

Future works can involve the development of new correlations to predict flooding and entrainment associated with additional error reductions, the utilization of neural networks to substitute the correlations available in the literature, and the development of a comparison of the proposed results with outputs obtained using commercial simulators for sieve tray columns.

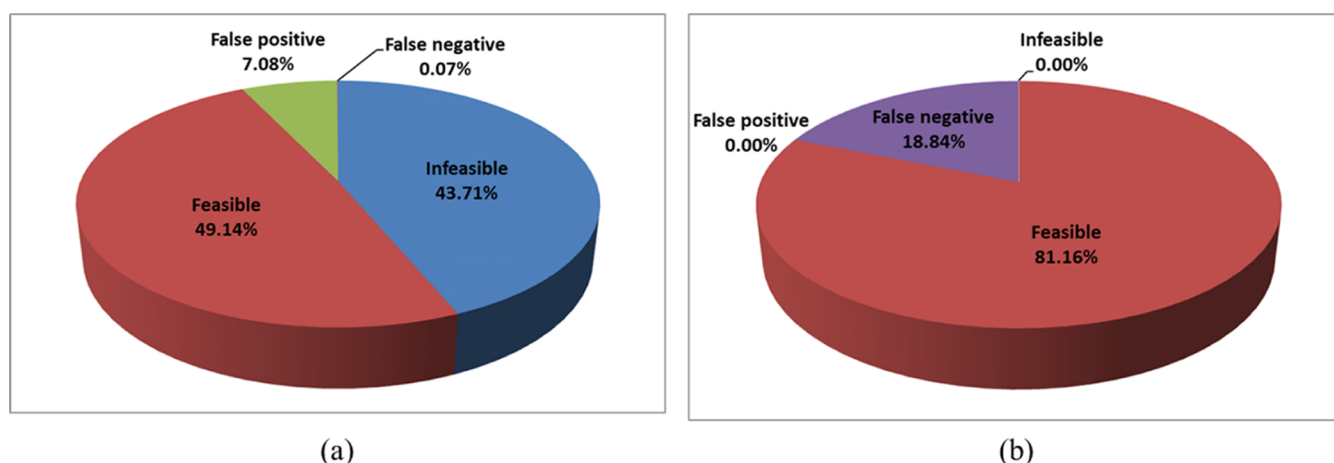


Figure 16. Example 1—Comparison between correlations of the Economopoulos<sup>8</sup> and our predictions—(a) flooding and (b) entrainment.

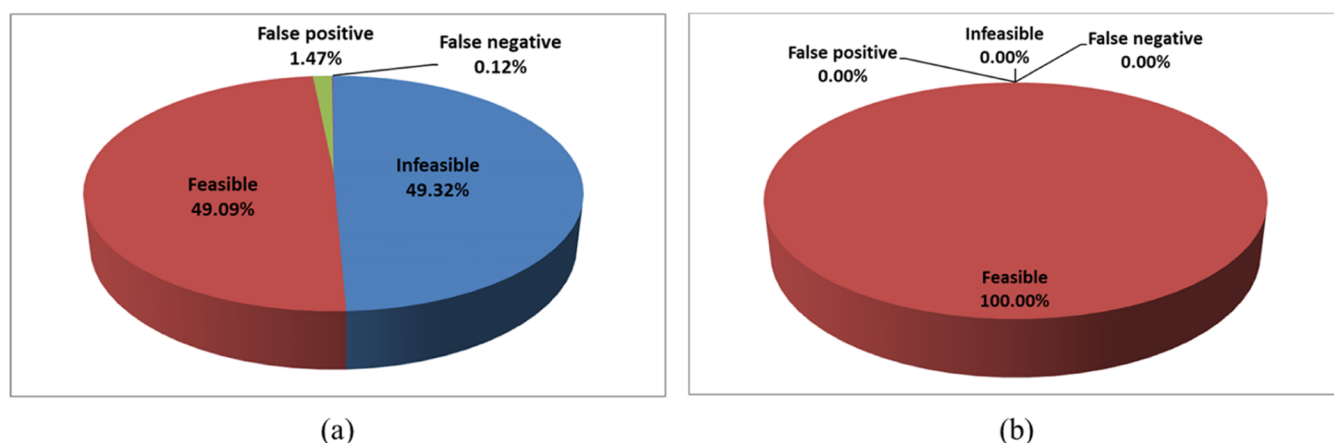


Figure 17. Example 1—Comparison between correlations of the Ogboja and Kuye<sup>11</sup> and our readjusted correlations—(a) flooding and (b) entrainment.

## ■ ASSOCIATED CONTENT

### SI Supporting Information

The Supporting Information is available free of charge at <https://pubs.acs.org/doi/10.1021/acs.iecr.4c03115>.

Digitalized points of Fair's curves; computational data about the parameter estimation problem; and results of parameter estimation without domain split and distillation design examples (PDF)

## ■ AUTHOR INFORMATION

### Corresponding Author

André L. H. Costa — Rio de Janeiro State University (UERJ), 20550-900 Rio de Janeiro, RJ, Brazil; [orcid.org/0000-0001-9167-8754](https://orcid.org/0000-0001-9167-8754); Email: [andrehc@uerj.br](mailto:andrehc@uerj.br)

### Authors

Aline R. C. Souza — Rio de Janeiro State University (UERJ), 20550-900 Rio de Janeiro, RJ, Brazil

Miguel J. Bagajewicz — Rio de Janeiro State University (UERJ), 20550-900 Rio de Janeiro, RJ, Brazil; School of Chemical, Biological and Materials Engineering, University of Oklahoma, Norman, Oklahoma 73019, United States; Federal University of Rio de Janeiro (UFRJ), Escola de Química, 21949-900 Rio de Janeiro, RJ, Brazil; [orcid.org/0000-0003-2195-0833](https://orcid.org/0000-0003-2195-0833)

Complete contact information is available at:

<https://pubs.acs.org/doi/10.1021/acs.iecr.4c03115>

### Funding

The Article Processing Charge for the publication of this research was funded by the Coordination for the Improvement of Higher Education Personnel - CAPES (ROR identifier: 00x0ma614).

### Notes

The authors declare no competing financial interest.

## ■ ACKNOWLEDGMENTS

A.R.C.S. thanks the Coordination for the Improvement of Higher Education Personnel (CAPES) for the scholarship. A.L.H.C. thanks the National Council for Scientific and Technological Development (CNPq) for the research productivity fellowship (Process 308727/2022-3) and the financial support of the Prociência Program (UERJ). M.J.B. thanks the visiting researcher scholarship from UERJ (PAPD Program) for part of the time of the development of this work.

## ■ NOMENCLATURE

$C_{sb}$  Souders–Brown coefficient (m/s, ft/s)  
 $D_c$  column diameter (m)  
 $d_h$  hole diameter (m)  
 $F_{flood}$  factor of flooding (dimensionless)

Flv	liquid–vapor flow factor (dimensionless)
$F_{\text{obj}}$	objective function (dimensionless)
hdwarp	difference between weir and clearance height under the downcomer (m)
hw	weir height (m)
$K$	constant of Fair flooding correlation (dimensionless)
$L$	liquid mass flow rate (kg/s)
lay	hole layout
lp	hole pitch (m)
lt	tray spacing (m, in)
lw	weir length (m)
tt	tray thickness (m)
uflood	flooding velocity (m/s)
un	vapor flow velocity (m/s)
$V$	vapor mass flow rate (kg/s)
$\mathbf{x}_i$	vector of the independent variable values at the data point $i$ (dimensionless)
$y_i^{\text{graph}}$	data obtained from the Fair's graph (dimensionless)
$y_i^{\text{model}}$	data obtained from the model (dimensionless)

## GREEK SYMBOLS

$\psi$	fractional entrainment (kg/kg gross liquid flow)
$\rho_l$	specific mass of liquid (kg/m <sup>3</sup> )
$\rho_v$	specific mass of vapor (kg/m <sup>3</sup> )
$\sigma$	surface tension (N/m)
$\sigma_{y,i}^2$	variance of the data points (dimensionless)
$\theta_{C_{\text{sb},k}}$	flooding correlation parameters (dimensionless)
$\theta_{\psi,k}$	entrainment correlation parameters (dimensionless)

## REFERENCES

- (1) Wankat, P. C. *Separations in Chemical Engineering: Equilibrium Staged Separations*; Elsevier: New York, 1988.
- (2) Kister, H. Z. *Distillation Design*, 1st ed.; McGraw-Hill, Inc.: New York, 1992.
- (3) Towler, G.; Sinnott, R. *Chemical Engineering Design Principles: Practice and Economics of Plant and Process Design*, 2nd ed.; Elsevier: Oxford, 2013.
- (4) Fair, J. R. How to Predict Sieve Tray Entrainment and Flooding. *Petro/Chem. Eng.* **1961**, 33 (10), 45–52.
- (5) Fair, J. R. Tray Hydraulics: Perforated Trays. In *Design of Equilibrium Stage Processes*; Smith, B. D., Ed.; McGraw-Hill: New York, 1963; pp 539–569.
- (6) Coulson, J. M.; Richardson, J. F.; Sinnott, R. K. *Chemical Engineering Design*, 4th ed.; Elsevier Butterworth-Heinemann: Oxford, 2005; Vol. 6.
- (7) Kister, H. Z.; Mathias, P. M.; Steinmeyer, D. E.; Penney, W. R.; Crocker, B. B.; Fair, J. R. Section 14 Equipment for Distillation, Gas Absorption, Phase Dispersion, and Phase Separation. In *Perry's Chemical Engineers' Handbook*; Green, D. W.; Perry, R. H., Eds.; McGraw-Hill Education: New York, 2008; pp 1–129.
- (8) Economopoulos, A. P. Computer Design of Sieve Trays and Tray Columns. *Chem. Eng.* **1978**, 85 (27), 109–120.
- (9) Lygeros, A. I.; Magoulas, K. G. Column Flooding and Entrainment. *Hydrocarbon Process.* **1986**, 65, 43–44.
- (10) Kessler, D. P.; Wankat, P. C. Correlations for Column Parameters. *Chem. Eng.* **1988**, 72–74.
- (11) Ogboja, O.; Kuye, A. A Procedure for the Design and Optimization of Sieve Trays. *Chem. Eng. Res. Des.* **1990**, 68 (5), 445–452.
- (12) Al-Baghli, N. A.; Pruess, S. A.; Yesavage, V. F.; Selim, M. S. A Rate-Based Model for the Design of Gas Absorbers for the Removal of CO<sub>2</sub> and H<sub>2</sub>S Using Aqueous Solutions of MEA and DEA. *Fluid Phase Equilib.* **2001**, 185 (1–2), 31–43.
- (13) Bansal, V.; Ross, R.; Perkins, J. D.; Pistikopoulos, E. N. The Interactions of Design and Control: Double-Effect Distillation. *J. Process Control* **2000**, 10 (2–3), 219–227.
- (14) Georgiadis, M. C.; Schenk, M.; Pistikopoulos, E. N.; Gani, R. The Interactions of Design Control and Operability in Reactive Distillation Systems. *Comput. Chem. Eng.* **2002**, 26 (4–5), 735–746.
- (15) Miranda, M.; Reneaume, J. M.; Meyer, X.; Meyer, M.; Szigeti, F. Integrating Process Design and Control: An Application of Optimal Control to Chemical Processes. *Chem. Eng. Process.* **2008**, 47 (11), 2004–2018.
- (16) Bansal, V.; Perkins, J. D.; Pistikopoulos, E. N. A Case Study in Simultaneous Design and Control Using Rigorous, Mixed-Integer Dynamic Optimization Models. *Ind. Eng. Chem. Res.* **2002**, 41 (4), 760–778.
- (17) Boukouvalas, C.; Magoulas, K.; Tassios, D. Application of Supercritical Fluid Extraction in Industrial Waste Treatment: Thermodynamic Modeling and Design. *Sep. Sci. Technol.* **1998**, 33 (3), 387–410.
- (18) Pereira, F. E.; Keskes, E.; Galindo, A.; Jackson, G.; Adjiman, C. S. Integrated Solvent and Process Design Using a SAFT-VR Thermodynamic Description: High-Pressure Separation of Carbon Dioxide and Methane. *Comput. Chem. Eng.* **2011**, 35 (3), 474–491.
- (19) Jachimović, B. M.; Genić, S. B.; Djordjević, D. R.; Budimir, N. J.; Jarić, M. S. Estimation of the Number of Trays for Natural Gas Triethylene Glycol Dehydration Column. *Chem. Eng. Res. Des.* **2011**, 89 (6), 561–572.
- (20) Chen, Y.; Gani, R.; Kontogeorgis, G. M.; Woodley, J. M. Integrated Ionic Liquid and Process Design Involving Azeotropic Separation Processes. *Chem. Eng. Sci.* **2019**, 203, 402–414.
- (21) Chávez-Islas, L. M.; Heard, C. L. Design and Analysis of an Ammonia/Water Absorption Refrigeration Cycle by Means of an Equation-Oriented Method. *Ind. Eng. Chem. Res.* **2009**, 48 (4), 1944–1956.
- (22) Taylor, R.; Kooijman, H. A.; Hung, J. S. A Second Generation Nonequilibrium Model for Computer Simulation of Multicomponent Separation Processes. *Comput. Chem. Eng.* **1994**, 18 (3), 205–217.
- (23) Souza, A. R. C.; Bagajewicz, M. J.; Costa, A. L. H. Globally Optimal Distillation Tray Design Using a Mathematical Programming Approach. *Chem. Eng. Res. Des.* **2022**, 180, 1–12.
- (24) Mitchell, M.; Muftakhidinov, B.; Winchen, T.; Jędrzejewski-Szmek, Z. Engauge Digitizer: Extracts Data Points from Images of Graphs, 2019. <https://markumtmitchell.github.io/engauge-digitizer/>.
- (25) Misener, R.; Floudas, C. A. ANTIGONE: Algorithms for coNTinuous/Integer Global Optimization of Nonlinear Equations. *J. Glob. Optim.* **2014**, 59 (2–3), 503–526.
- (26) Drud, A. CONOPT: A GRG Code for Large Sparse Dynamic Nonlinear Optimization Problems. *Math. Program.* **1985**, 31 (2), 153–191.
- (27) Sahinidis, N. V. BARON: A General Purpose Global Optimization Software Package. *J. Glob. Optim.* **1996**, 8 (2), 201–205.
- (28) Nelder, J. A.; Mead, R. A Simplex Method for Function Minimization. *Comput. J.* **1965**, 7 (4), 308–313.
- (29) Spendley, W.; Hext, G. R.; Himsforth, F. R. Sequential Application of Simplex Designs in Optimisation and Evolutionary Operation. *Technometrics* **1962**, 4 (4), 441–461.
- (30) Kennedy, J.; Eberhart, R. Particle Swarm Optimization. In *Proceedings of ICNN'95—International Conference on Neural Networks*; IEEE: Perth, WA, Australia, 1995; Vol. 4, pp 1942–1948.
- (31) Kiss, A. A.; Ignat, R. M. Enhanced Methanol Recovery and Glycerol Separation in Biodiesel Production—DWC Makes It Happen. *Appl. Energy* **2012**, 99, 146–153.
- (32) Costa, A. L. H.; Bagajewicz, M. J. 110th Anniversary: On the Departure from Heuristics and Simplified Models toward Globally Optimal Design of Process Equipment. *Ind. Eng. Chem. Res.* **2019**, 58 (40), 18684–18702.
- (33) Souza, A. R. C.; Bagajewicz, M. J.; Costa, A. L. H. Set Trimming Approach for the Globally Optimal Design of Sieve Trays in Separation Columns. *AIChE J.* **2023**, 69 (5), 1–14.